Laporan Akhir Projek Penyelidikan Jangka Pendek

Fabrication of carbon Nanotube Filled Polydimethylsilozane (PDMS) Composites and Its Behavior as Thermal Interface Material (TIM) in Electronic Packaging

By
Prof. Ir. Dr. Mariatti Bt. Jaafar @ Mustapha

Final Report

"Fabrication of Carbon Nanotubes Filled Polydimethysilozane (PDMS) Composites and its Behavior as Thermal Interface Material (TIM) in Electronic Packaging"

1. Introduction

Silicone rubbers are found to be useful in numerous products, applications, and processes across all industries. This is because silicone rubbers possess unique physical, chemical and mechanical properties that are unmatched by any other polymeric materials. Among the properties of silicone rubbers are low surface tension, hydrophobicity, chemical resistance, electrical insulation, resistance to weathering, stability to extreme temperatures, resistance to thermal shock, high elasticity, good tear strength, capability to seal or bond materials of various natures, and so on. However, unfilled silicone rubbers usually have low mechanical, electrical and thermal conductive properties. That is why silicone rubbers are often combined with fillers such as metal powders, fumed and precipitated silica, carbon black, boron nitride and zinc oxide to improve the above-mentioned properties.

For many years, there have been extensive research on silicone rubber-based composites, for which the attentions were mostly towards the thermal properties of the materials (1-3). With the advancement in electronics technology, miniaturization of transistors which allow more transistors to be integrated into a single device is made possible. Nevertheless, integration and cramming of transistors will increase power usage and heat flux at the device. Thus, heat dissipation issue becomes a great importance, and it is very crucial for the heat generated from the device to be dissipated as quickly and effectively as possible. Else, the operating temperatures of the device will not be optimum, and it will reduce the lifespan of the device (1-3).

Traditionally, to solve the heat dissipation problem, a heat sink is embedded to the device. Relying on the heat sink alone to dissipate heat is not enough due to interfacial thermal resistance arising from non-surface flatness and surface roughness of both device and heat sink. This resulted about 99% of the interfaces being separated by air gaps, which significantly reduce the capability to dissipate heat due to the poor thermal conductivity of air. Thus, an additional material, called the Thermal Interface Material (TIM) is employed between the two materials to reduce thermal contact resistance and provide effective heat conduction (3). There were quite a number of researches dealing with effect of fillers on the thermal conductivity of silicone rubber. Zhou et al. (2) had reported in two separate papers that boron nitride-silicone rubber and silicon nitride-silicone rubber systems had shown a significant increase in thermal conductivity. They also reported in another paper that the thermal conductivity of silicone rubber increased with increasing alumina concentration up to 80 vol%. On the other hand, Liu et al. (4) reported an enhancement of 65% in thermal conductivity with 4 wt% carbon nanotube (CNT) loading in silicone rubber.

Carbon nanotubes (CNTs) are new-type carbon materials that exhibit excellent mechanical properties (5). CNTs consist of folded graphene layers with cylindrical hexagonal lattice structure (6). The length of a CNT is from a few microns up to a few millimetres, with a

diameter of the order of nanometers. A single carbon nanotube is hundred times stronger and six times lighter than steel and exhibits good electrical and thermal conductivities. With only a low concentration to improve the properties of the composite, it is clear that carbon nanotube (CNTs) have attracted a great deal of interest and are the most talk about polymer composite fillers among researchers. Comparing with the enormous number of studies on the application of CNTs in epoxies, thermoplastics and fibers, there are rather few reports dealing with applications of CNTs in rubber (7). Since both silicone rubbers and CNTs have their own unique and excellent properties, it is believed that combining these two groups of materials can lead to a very attractive and multifunctional composite that can find extensive application in many fields. The addition of CNTs into polydimethylsiloxane (PDMS), a type of silicone elastomer, has been reported to have improved the mechanical, electrical and thermal properties of the composites. Wu et al. (8) reported that the elastic modulus of PDMS/CNT composite increases when 2.0 wt% CNTs are added into the PDMS matrix. Furthermore, the storage modulus and hardness also increased with the addition of CNTs. In a separate work, Hong et al. (9) revealed that the thermal conductivity of PDMS composite increases with filler loading.

There is minimal research on the effect of processing methods on the properties of PDMS nanocomposites filled with multi-walled carbon nanotubes (MWCNTs). The current work aims to compare the properties of PDMS/MWCNTs nanocomposites produced by two different methods: solution mixing and mini-extruder. Solution mixing is a common method, as it has been widely used by many researchers. On the other hand, the mini-extruder method is considered a new approach, although its mechanism is based on shear mixing. In this research, the effect of MWCNT loading on the properties of PDMS/MWCNTs nanocomposites was also studied.

2. Experimental

2.1 Materials

PDMS (Sylgard 182 Silicone Elastomer), consisting of a base elastomer (Part A) and a curing agent (Part B), was purchased from Dow Corning, USA. MWCNTs 40–60 nm in diameter and 100 nm in length with 90–95% purity were purchased from Shenzhen Nanotech Port Co., Ltd., China. The solvent used to disperse the MWCNTs was toluene (99.9%) purchased from J.T. Baker.

2.2 Fabrication of PDMS/MWCNTs nanocomposites via solution mixing method

The parameters used in this method were based on our previous work (10). The MWCNTs were first dispersed in 25 ml of toluene and sonicated in an ultrasonic bath for 30 min. Part A of the PDMS was then added to the suspension of MWCNTs and toluene. The mixture was stirred using a mechanical stirrer at 400 rpm and 70°C for 1 h to allow the toluene to evaporate. When the toluene was fully removed, the mixture was allowed to cool to room temperature to avoid rubber cross-linking upon adding the curing agent. Part B was then added to the mixture (Part A and MWCNTs) in the ratio of 10:1 (Part A: Part B). The Part A, Part B, and MWCNT mixture and curing agent were further stirred using a mechanical stirrer at 800 rpm and room temperature for 10 min. The mixture was then cast into a 1 mm thick mold plate and was degassed in a vacuum for 1 h. It was then compressed using cold press machine (70 kg/cm^2) for

1 min. Subsequently, the compressed mixture was cured in an oven at 150°C for 2 h. By using a similar procedure, nanocomposites with nanotube loadings of 1, 2, 3, and 4 wt% were prepared. Nanocomposites prepared using this method hereafter will be called nanocomposites A.

2.3 Fabrication of PDMS/MWCNTs nanocomposites using the mini-extruder

MWCNTs were mixed with Part A (PDMS) using the DSM Micro 15 cm^3 mini-extruder for 10 min at room temperature. Screw rotating speed was set to 200 rpm. Part B was then added to the mini-extruder and was mixed for an additional 10 min at room temperature using the same rotating speed as before. Here, the ratio of Part A to Part B was fixed at 10:1. The mixture was extruded out, placed into a 1 mm thick mold plate, and degassed in a vacuum for 1 h. The mixture was then pressed and cured simultaneously at 150°C for 2 h via hot press. Nanocomposites with nanotube loadings of 1, 2, 3, and 4 wt% were prepared using similar procedures as those for 0% nanotubes. Nanocomposites prepared using this method hereafter will be called nanocomposites B.

2.4 Characterization of PDMS/MWCNTs nanocomposites

The viscosity of uncured mixture (PDMS and MWCNTs) was determined with the Brookfield DV-II+ Viscometer using the RV3 spindle at a rotating speed of 5 rpm. Tensile test was conducted using the Instron 3366 Universal Testing Machine. The fracture surface of the nanocomposites was observed using the FEI Quanta 3D Environmental Scanning Electron Microscope. The electrical conductivity of the nanocomposites was measured using the Advantest R8340 Ultra High Resistance Meter. This test was carried out at room temperature with a constant voltage of 500 V. The thermal conductivity of the nanocomposites was obtained using the Hot Disk Thermal Constant Analyzer (TPS 2500S) with a constant power of 0.7 W. Thermogravimetric analysis (TGA) was carried out to study the thermal stability of the nanocomposites. The test was conducted using Perkin Elmer's Pyris™ 6 TGA, heating from room temperature to 800°C (heating rate: 10°C/min) in nitrogen atmosphere. The glass transition temperature (T_g) and coefficient of thermal expansion of the nanocomposites were determined using the Perkin Elmer TMA7 Thermomechanical Analyzer. The sample was heated from -150°C to 250°C at a heating rate of 5°C/min and was purged in nitrogen gas at a rate of 30 ml/min.

3. Results and Discussion

3.1 Characterization of Raw Materials

3.1.1 Surface Morphology of Fillers

The TEM images of pristine MWCNT (MWCNT-p) and functionalized MWCNTs are shown in Figures 1(a), 1(b), and 1(c). Figure 1(a) reveals that the wall of the pristine MWCNT is smooth and no extra phase is observed. In contrast, the walls of both functionalized MWCNTs are heterogeneous, rough and strained with extra substances, as can be seen in Figures 3.1(b) and 3.1(c). This is believed to be due to acidic etching of the nanotubes surface during chemical (acid) treatment to induce the functional groups (11).

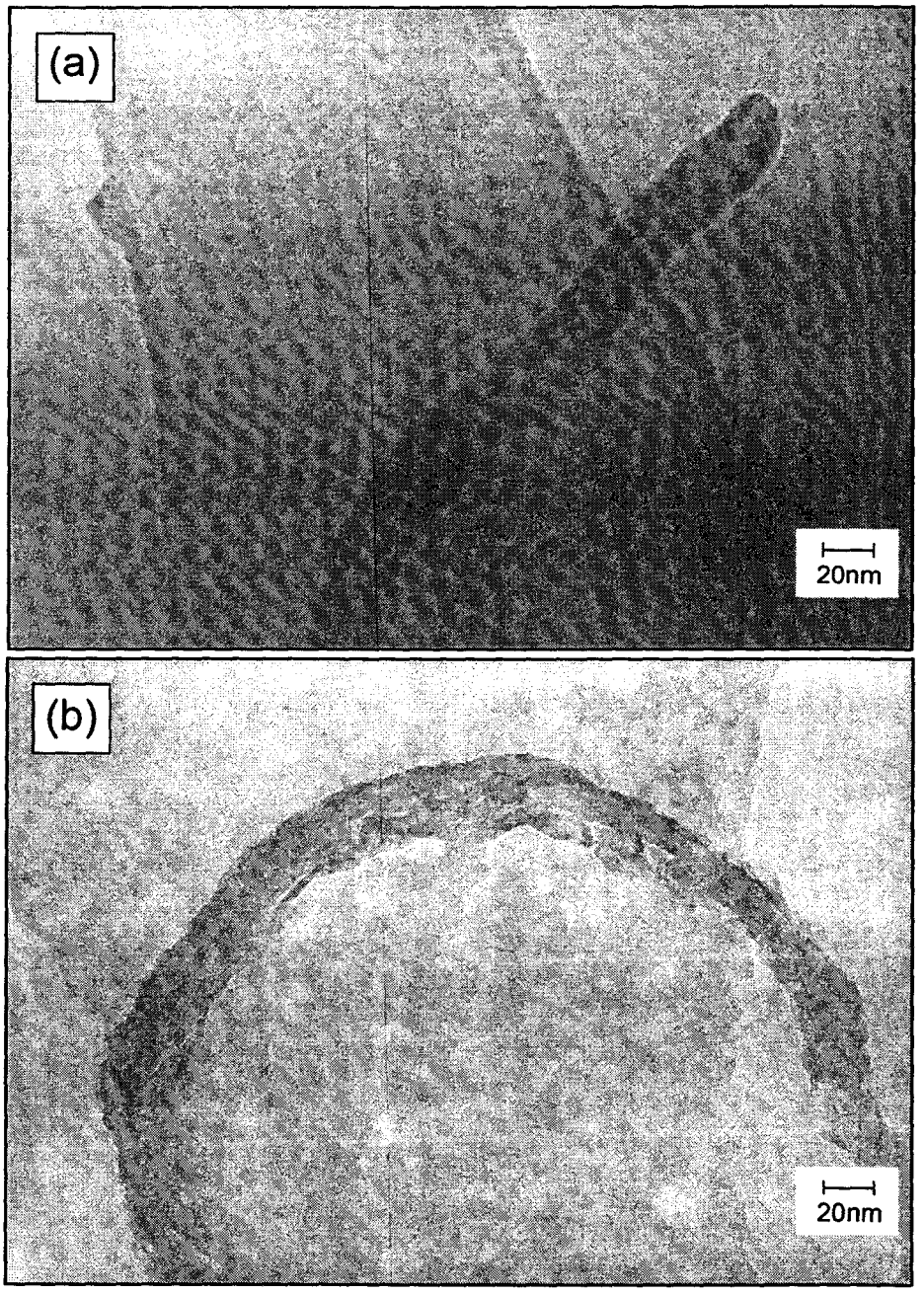

Figure 1: TEM micrographs of (a) MWCNT-p, (b) MWCNT-OH, and (c) MWCNT-COOH

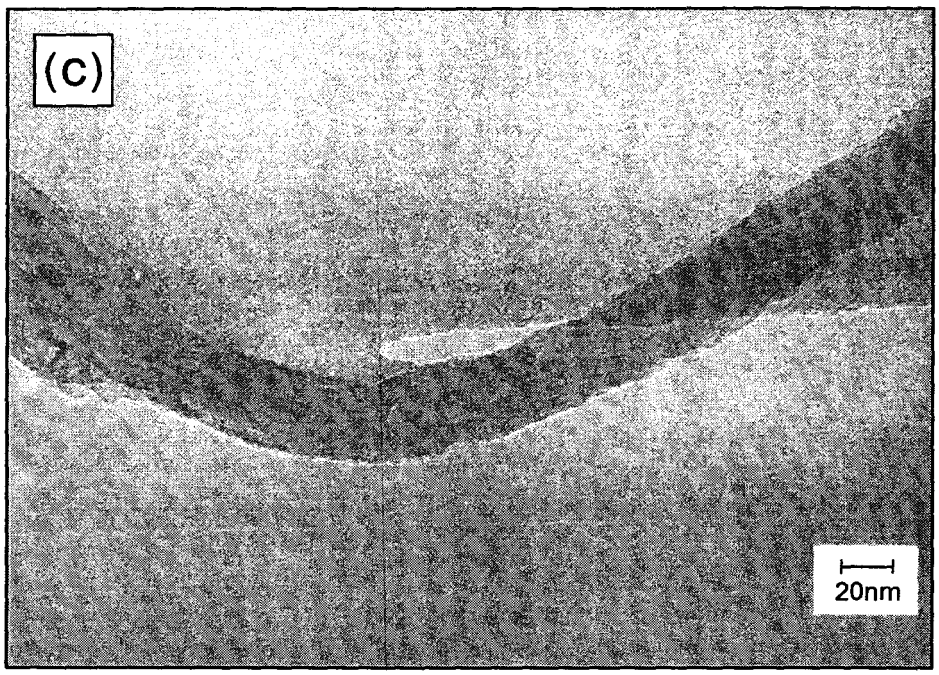

Figure 1: TEM micrographs of (a) MWCNT-p, (b) MWCNT-OH and (c) MWCNT-COOH. *(Continued).*

3.1.2 Raman Spectroscopy Analysis of MWCNTs

The Raman spectra of pristine and functionalized MWCNTs are shown in Figure 2. The MWCNTs display two characteristic peaks at approximately 1340 and 1570 cm^{-1}, termed as *D*-band and *G*-band, respectively. The *G*-band relates to the structural intensity of the sp^2-hybridized carbon atoms of CNTs, whereas the *D*-band reflects disorder-induced carbon atoms resulting from the defects in CNTs and their ends (12, 13). The intensity of *D*-band is usually governed by the presence of amorphous carbon and graphitic impurities (14). The higher *D*-band intensity and the smaller *G*-band to *D*-band ratio (I_G/I_D) of both MWCNT-OH and MWCNT-COOH indicate a high degree of disorder and the presence of defects on the surface of the functionalized CNT resulting from chemical modification (12).

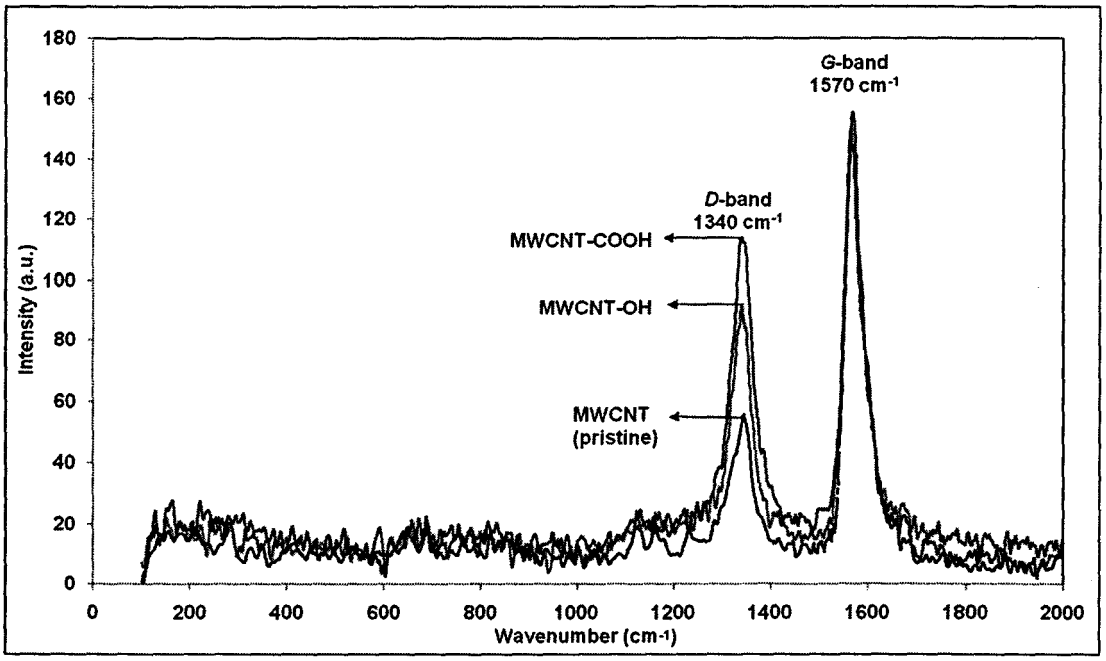

Figure 2: Raman spectra of pristine MWCNT-p, MWCNT-OH, and MWCNT-COOH.

3.2.3 Fourier Transform Infrared (FTIR) Spectroscopy Analysis of Fillers

The FTIR spectrums of the fillers studied (after smoothing and baseline correction) are shown in Figure 3. The MWCNT-p spectrum shows only one weak peak at the wavelength 3468 cm^{-1}, which is assigned to hydroxyl groups. This peak could be due to absorbed moisture attached to the nanotubes (13). The spectrum of MWCNT-OH shows three different peaks. The peak detected at 3415 cm^{-1}, which is also assigned to hydroxyl groups and attributed to stretching vibration of O-H, has higher and broad absorbance intensity as compared to MWCNT-p. The other two peaks detected at 1021 cm^{-1} and 1444 cm^{-1} are attributed to stretching vibration of C-OH and bending vibration of O-H, respectively. These observed peaks indicate that the –OH functional groups are present on the surface of nanotubes (14).

The MWCNT-COOH spectrum shows four characteristic peaks at 1073 cm^{-1}, 1428 cm^{-1}, 1737 cm^{-1}, and 3408 cm^{-1}. The peaks at 1073 cm^{-1}, 1428 cm^{-1}, and 3408 cm^{-1} are attributed to C-OH stretch, O-H bend, O-H stretch, respectively, which is similar to the ones observed in MWCNT-OH. The peak at 1737 cm^{-1} is attributed C=O stretch, indicating the presence of carboxyl groups.

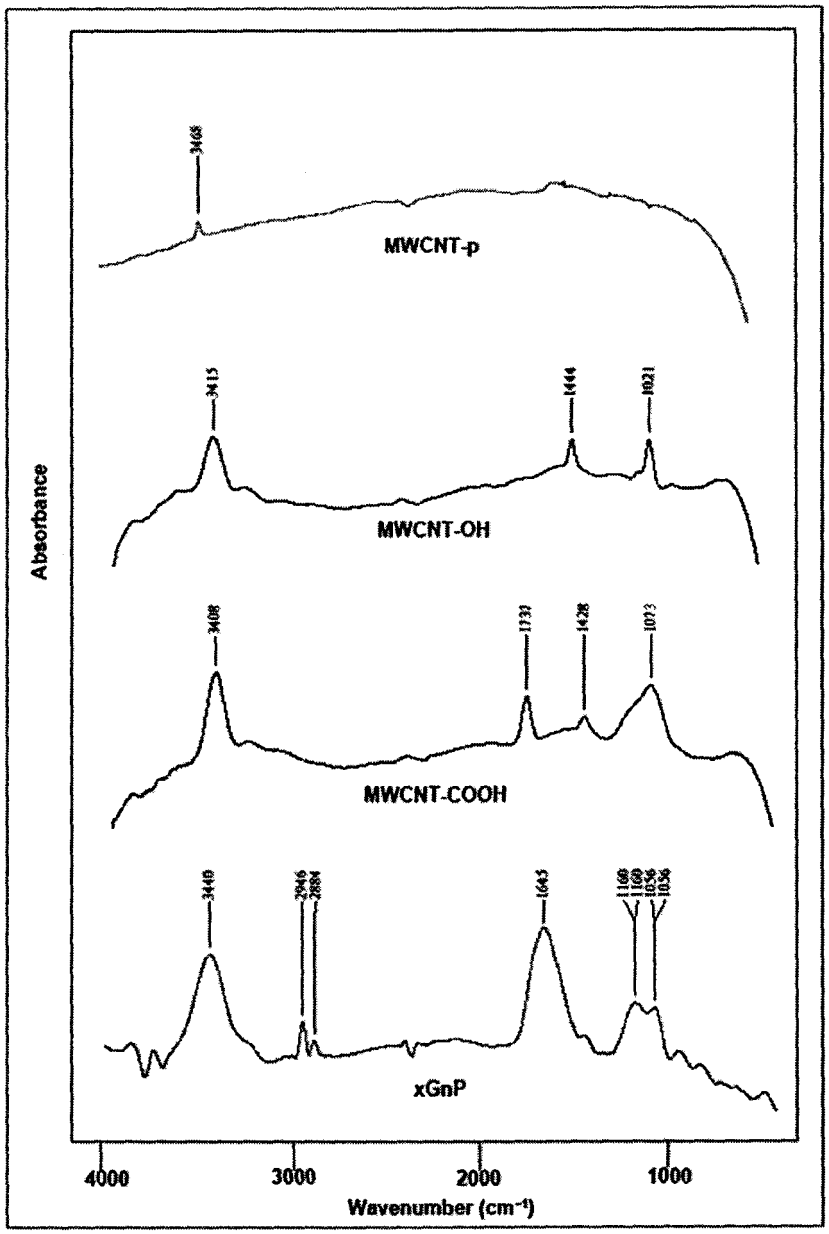

Figure 3: FTIR spectrums of MWCNT-p, MWCNT-OH, MWCNT-COOH, and xGnP.

3.2.4 Elemental Analysis of Fillers

The elemental analysis was carried out to determine the elemental composition of the as-received fillers. Figures 4(a), 4(b) and 4(c) show the Energy Dispersive X-Ray Spectroscopy (EDS) spectrums of MWCNT-p, MWCNT-OH and MWCNT-COOH, respectively while Table 1 summarize the composition of elements that are present in the fillers. All three fillers shows a high content of carbon (C), which is expected since they are carbon-based fillers. However, it is observed that MWCNT-p is composed entirely of C. Based on the data sheet provided by supplier, the purity of MWCNT-p is around 97%.

Both the MWCNT-OH and MWCNT-COOH contains C, oxygen (O), and nickel (Ni). The composition of C, O, and Ni in MWCNT-OH is 98.01 wt%, 0.61 wt%, and 1.38 wt%, respectively while the composition of C, O, and Ni in MWCNT-COOH is 97.62 wt%, 0.41 wt% and 1.97 wt%, respectively. The presence of O is due to the acid treatments involved to introduce functional groups on the surface of nanotubes. Ni is the catalyst used during the synthesis of MWCNTs via catalytic chemical vapor deposition (CCVD).

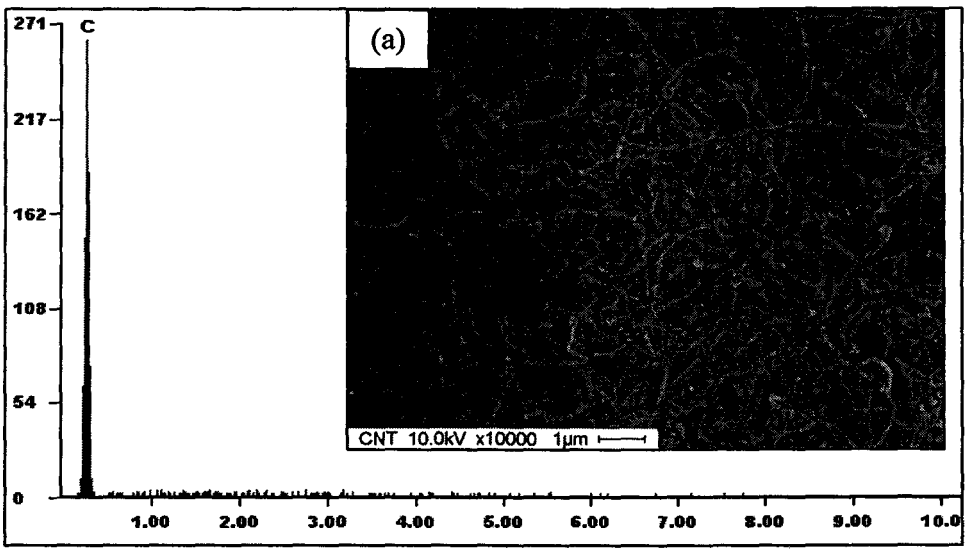

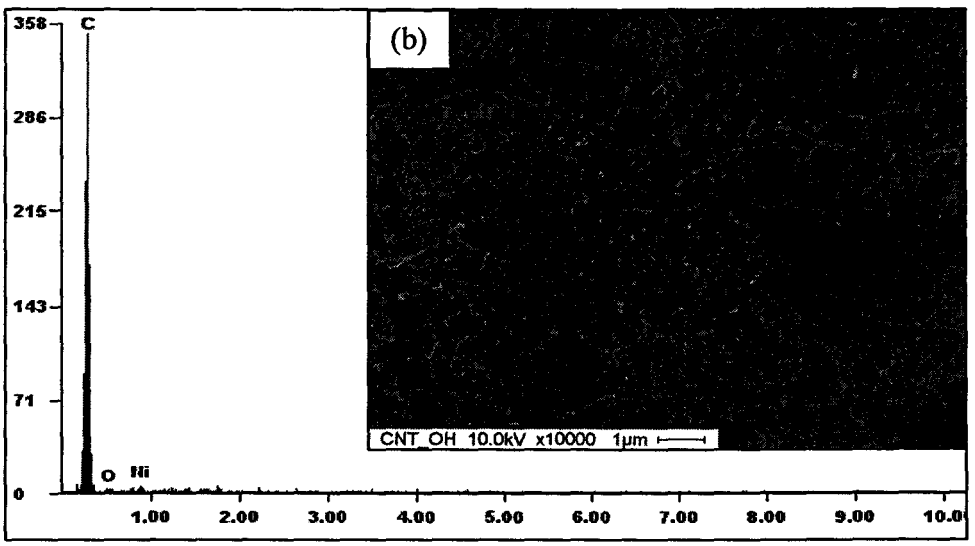

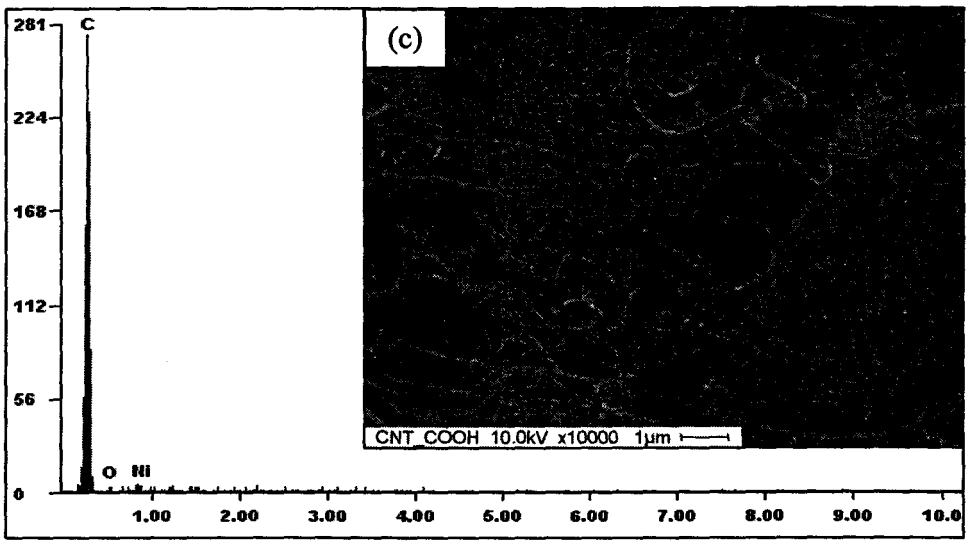

Figure 4: EDS spectrums and SEM images of (a) MWCNT-p, (b) MWCNT-OH, (c) MWCNT-COOH

Table 1: Composition of elements that are present in MWCNT-p, MWCNT-OH and MWCNT-COOH.

Filler	Composition (wt%)			
	C	O	Ni	S
MWCNT-p	100.00	-	-	-
MWCNT-OH	98.01	0.61	1.38	-
MWCNT-COOH	97.62	0.41	1.97	-

3.2.5 Thermal Stability of Fillers

Thermogravimetric analysis (TGA) was used to characterize the thermal stability of the fillers. Table 2 shows the decomposition temperature at 5% weight loss (T_5), 10% weight loss (T_{10}) and total weight loss at 800 °C. MWCNT-p is hardly decomposed and have good thermal stability with only 2.9% weight loss at 800 °C. This small amount of weight loss correspond to the decomposition of amorphous carbonaceous impurities that adhered on the surface of the regular graphitized walls (15).

The MWCNT-OH decompose slowly from 100 °C up to 700 °C. Major weight loss can only be seen after 700 °C and the total weight loss of MWCNT-OH at 800 °C is 30.1%. Similar

to MWCNT-OH, MWCNT-COOH also shows two decomposition steps. The first decomposition occurs from 50 - 550 °C and the second decomposition, which is a major one, occurs after 550 °C. The total weight loss for MWCNT-COOH at 800 °C is 34.5%. The large amount of weight loss and lower thermal stability of both functionalized MWCNTs as compared to the pristine MWCNTs has been reported and this can be attributed to the removal of functional groups (–OH and –COOH) attached to the nanotubes (16).

Table 2: Thermal stability data for MWCNT-p, MWCNT-OH, MWCNT-COOH, and xGnP, extracted from TGA curves.

Filler	Temperature (°C)		Total weight loss at 800 °C (%)
	T_5	T_{10}	
MWCNT-p	-	-	2.9
MWCNT-OH	712	754	30.1
MWCNT-COOH	578	648	34.5

T_5 and T_{10} represents decomposition temperature at 5% and 10% weight loss, respectively

3.3 Effect of Processing Methods on the Properties of PDMS/MWCNT Composites

3.3.1 Dispersion and Morphological Study of MWCNTs in PDMS

The dispersion of nanotubes in polymeric matrix is an important aspect to be considered in polymer/MWCNT composites as it affects majority of the composites properties. It is expected that the properties of PDMS/MWCNT composites will improve significantly when nanotubes are well-dispersed in PDMS matrix with minimal agglomerations. However, it poses a great challenge to disperse the nanotubes and prevent agglomerations as MWCNTs are highly entangled, partly due to the high aspect ratio of CNTs, as well as the van der Waals interactions among them.

Figure 5 presents the transmission mode optical microscope digital images of PDMS filled with 4 wt% pristine MWCNT composites produced by mini-extruder (M-PDMS/4 wt% MWCNT-p) and solution mixing method (S-PDMS/4 wt% MWCNT-p), illustrating the overall distribution and dispersion of MWCNTs in the matrices obtained from different processing methods. The nanotubes are represented as black-colored area while the PDMS polymer is represented as white-colored area. From Figure 5(a), it can be observed that the black area and white area are well distributed although a small amount of large black spots can also be observed. On the other hand, many large black spots can be seen in Figure 5(b), indicating the presence of large nanotubes agglomerates and clusters (marked by red circles). From both figures, it is deduced that composites produced by mini-extruder have relatively better dispersion of nanotubes in PDMS matrix. This is partly due to the high shear force of the rotating twin

screws which broke the large agglomerates of nanotubes into smaller bundles and subsequently dispersed the nanotubes easily.

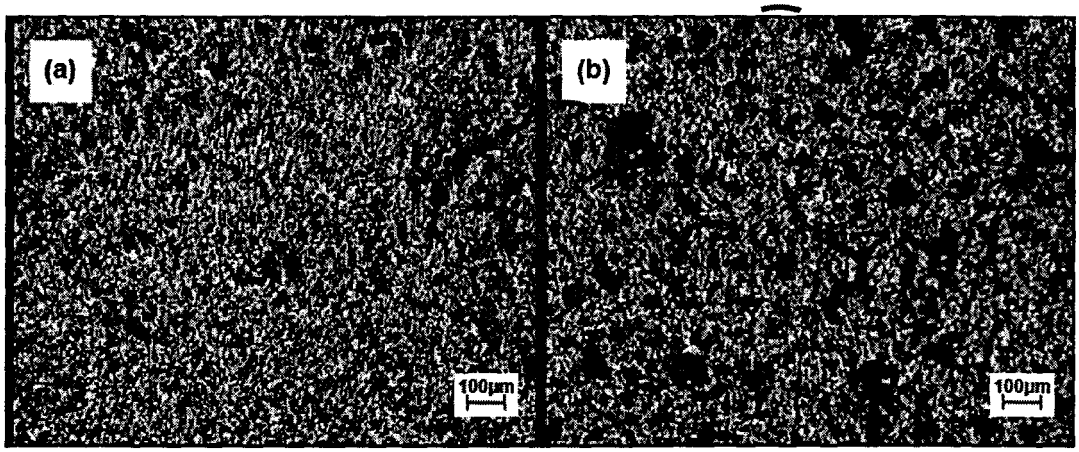

Figure 5: Transmission mode optical microscope digital images of 4 wt% pristine MWCNTs in PDMS composites produced by (a) mini-extruder and (b) solution mixing.

The fractured surface morphologies of PDMS filled with 1 wt% and 4 wt% pristine MWCNTs composites produced by mini-extruder and solution mixing method are shown in Figure 6, respectively. The figures provide some insight into the nanoscale dispersion state of MWCNTs. Composites produced by mini-extruder, represented by Figures 6(a), 6(b), and 6(e) show that the nanotubes are relatively better dispersed in PDMS although at higher filler loading, a few small agglomerates of nanotubes can be observed. Figures 6(c), 6(d), and 6(f) which represented composites produced by solution mixing, reveal the presence of large clusters and agglomerates of nanotubes in PDMS. For low filler loading (Figure 6(c) and 6(f)), agglomerates as large as 25 μm can be observed while for high filler loading (Figure 6(d)), clusters and agglomerates as large as 150 μm can be seen. This observation indicates that the dispersion of nanotubes in PDMS composite produced by mini-extruder is relatively better than the ones produced by solution mixing method, which is in agreement with the observations by optical microscope images (Figure 5).

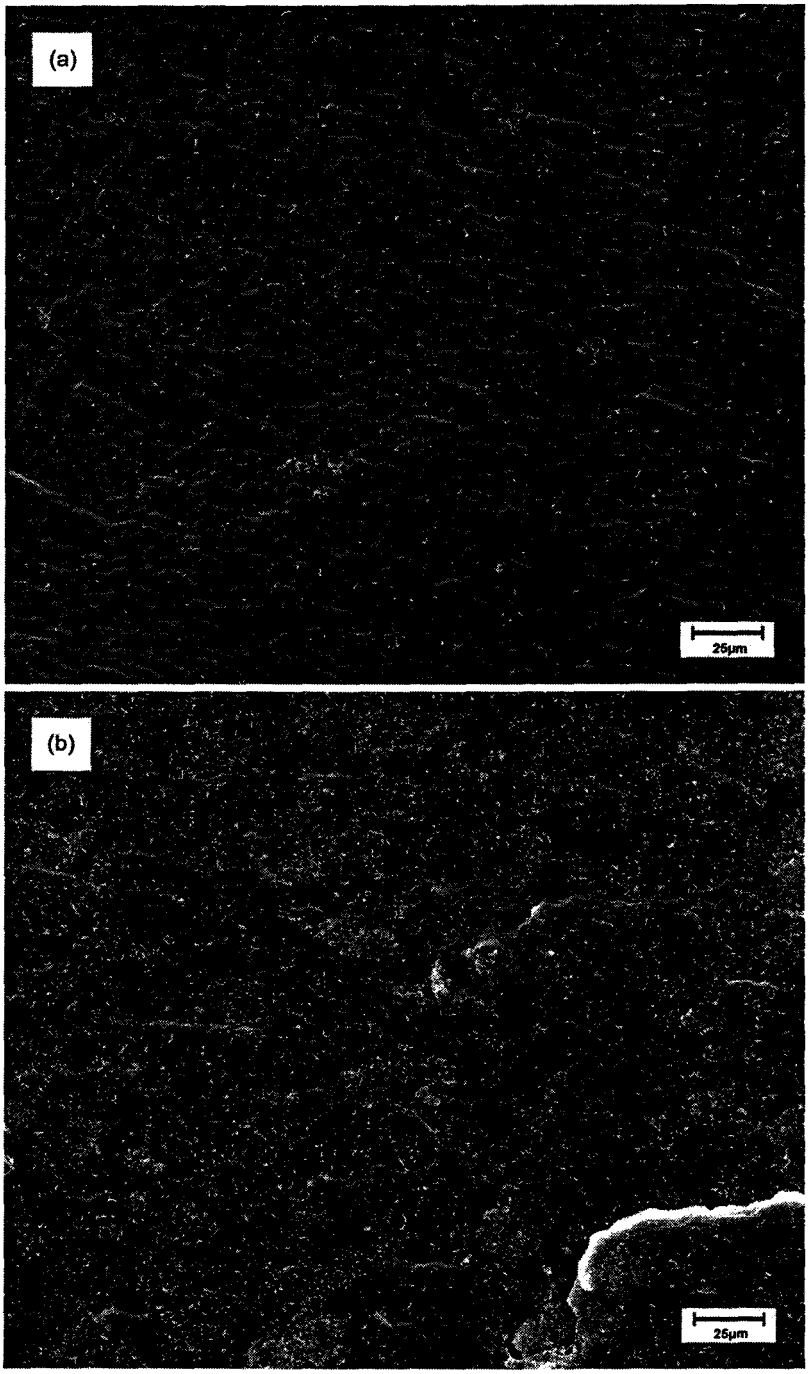

Figure 6: SEM micrographs on fractured surface of (a) M-PDMS/1 wt% MWCNT-p, (b) M-PDMS/4 wt% MWCNT-p, (c) S-PDMS/1 wt% MWCNT-p, (d) S-PDMS/4 wt% MWCNT-p, (e) M-PDMS/1 wt% MWCNT-p, and (f) S-PDMS/1 wt% MWCNT-p. (a)-(d) were taken at 1000x magnification while (e)-(f) were taken at 5000x magnification.

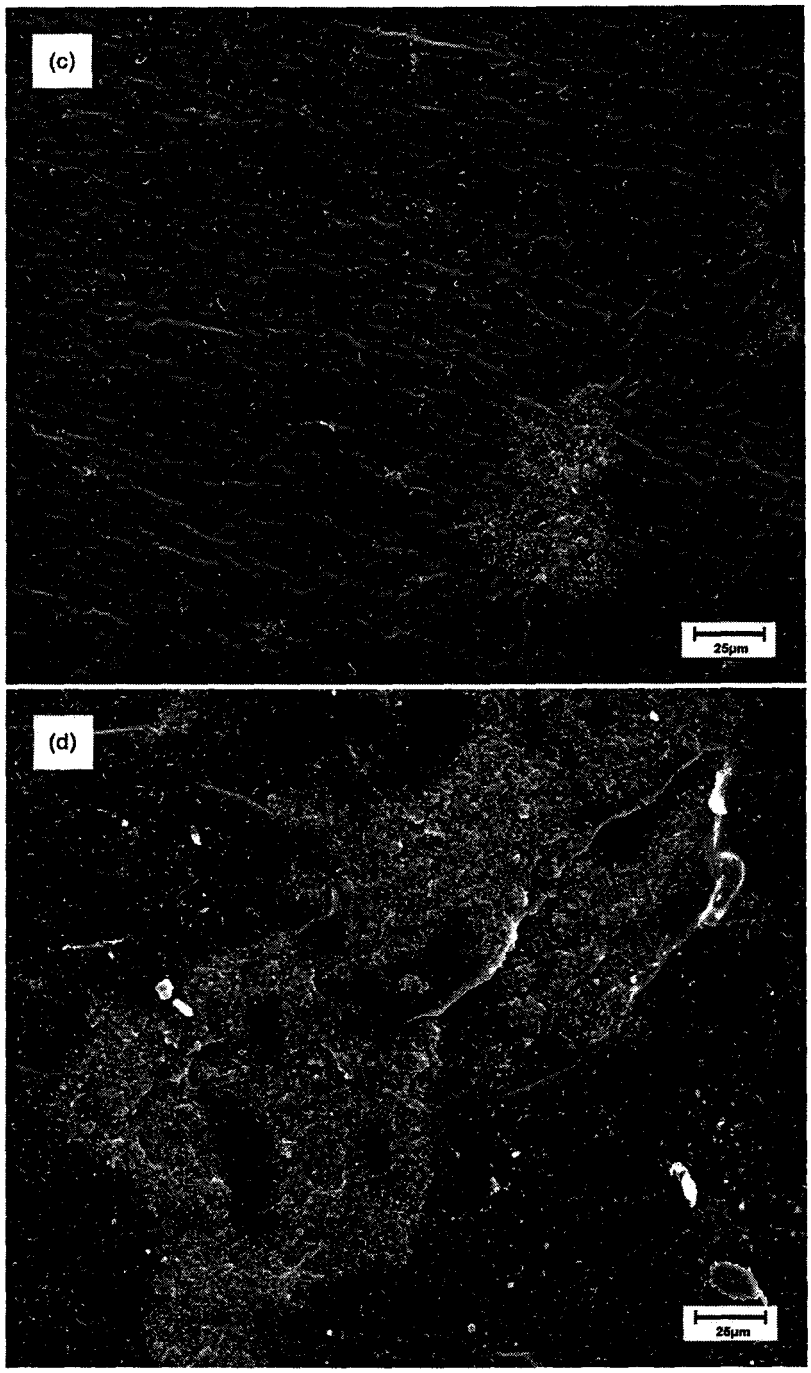

Figure 6: SEM micrographs on fractured surface of (a) M-PDMS/1 wt% MWCNT-p, (b) M-PDMS/4 wt% MWCNT-p, (c) S-PDMS/1 wt% MWCNT-p, (d) S-PDMS/4 wt% MWCNT-p, (e) M-PDMS/1 wt% MWCNT-p, and (f) S-PDMS/1 wt% MWCNT-p. (a)-(d) were taken at 1000x magnification while (e)-(f) were taken at 5000x magnification. *(Continued).*

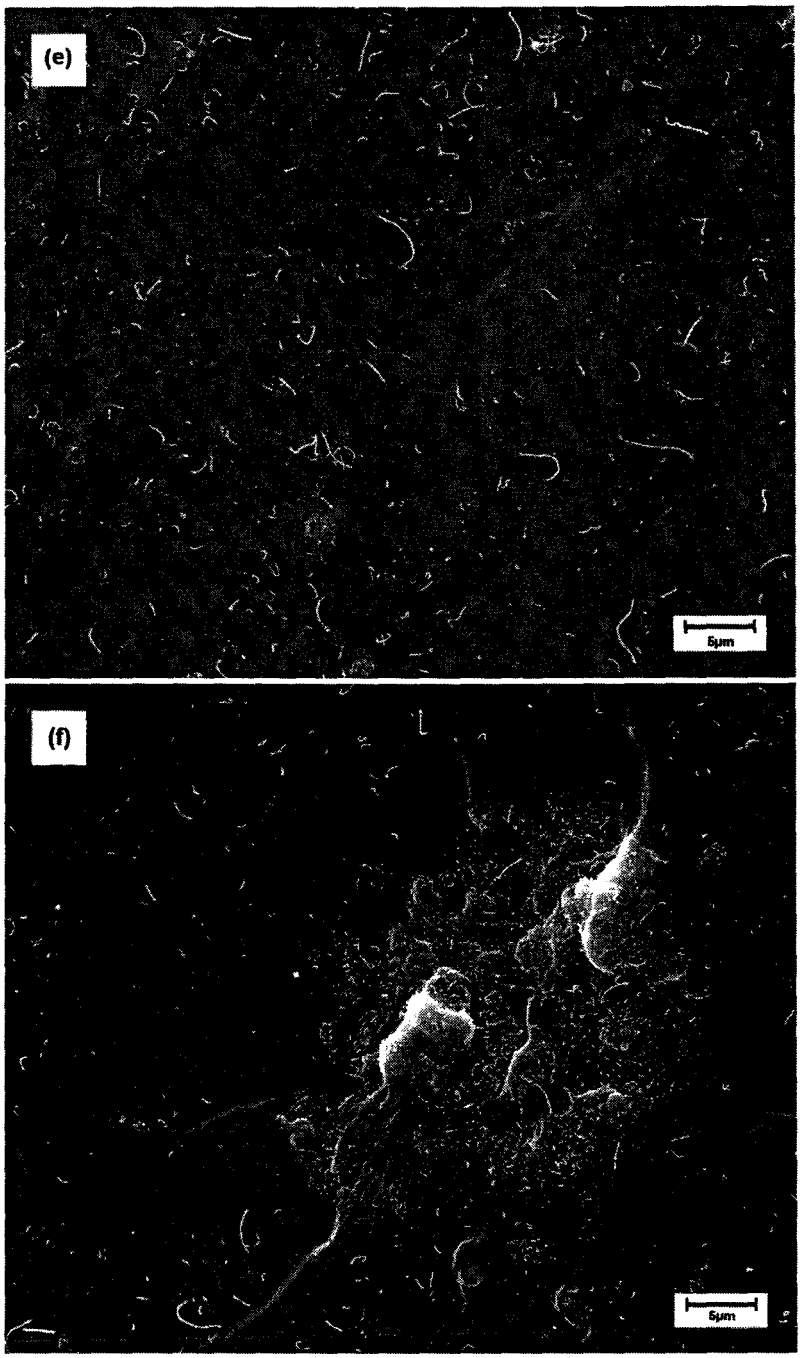

Figure 6: SEM micrographs on fractured surface of (a) M-PDMS/1 wt% MWCNT-p, (b) M-PDMS/4 wt% MWCNT-p, (c) S-PDMS/1 wt% MWCNT-p, (d) S-PDMS/4 wt% MWCNT-p, (e) M-PDMS/1 wt% MWCNT-p, and (f) S-PDMS/1 wt% MWCNT-p. (a)-(d) were taken at 1000x magnification while (e)-(f) were taken at 5000x magnification. *(Continued).*

Better dispersion of nanotubes in PDMS composite produced by mini-extruder is partly due to the mechanism involved during the mixing of nanotubes and PDMS. The high shearing force of the rotating twin-screw has chopped the nanotubes into shorter lengths. It is reported that shortened nanotubes can be dispersed more easily in polymeric matrix and this has been proven with SEM micrographs (17). As for the current work, SEM micrographs at 10000x magnification in Figure 7 show that the composites produced by mini-extruder have shorter nanotubes compared to the ones produced by solution mixing.

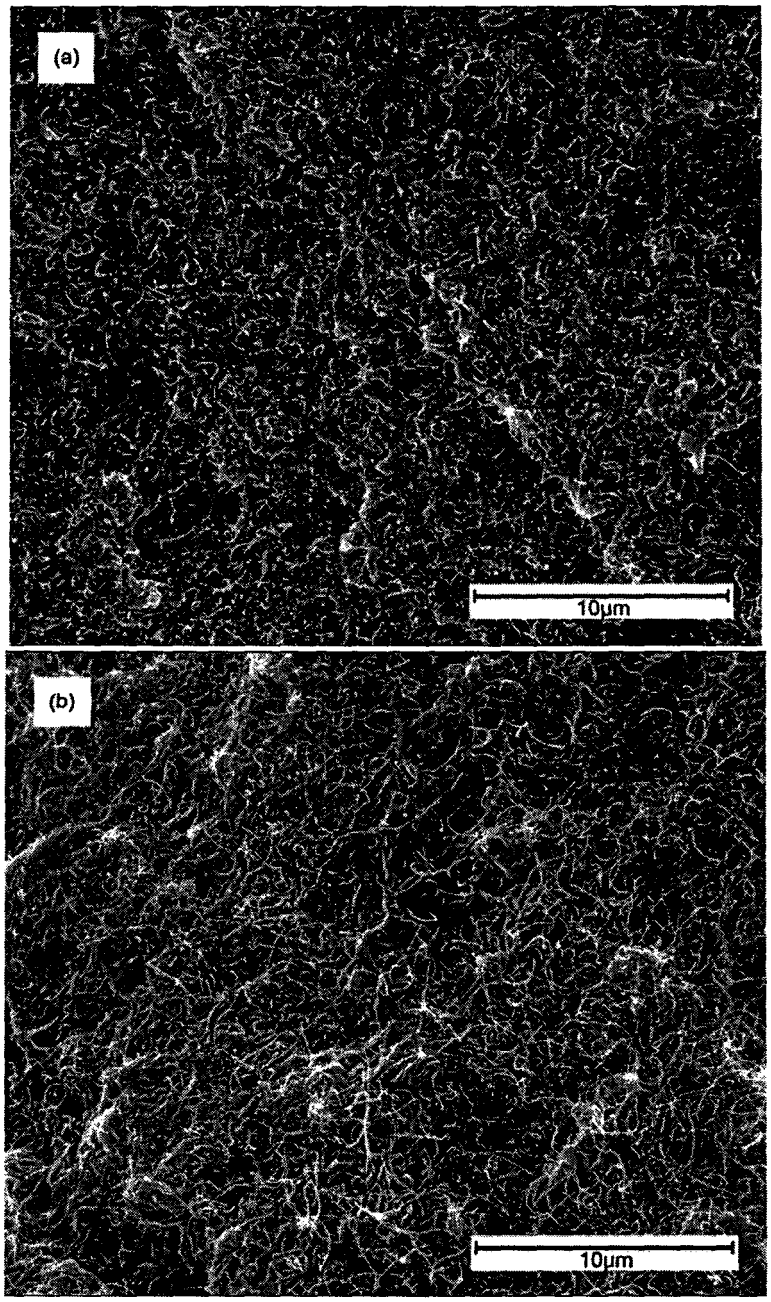

Figure 7: SEM micrographs of (a) M-PDMS/4 wt% MWCNT-p and (b) S-PDMS/4 wt% MWCNT-p at 10000x comparing the nanotubes length.

3.3.2 Crosslink Density

Crosslink density is an important factor governing the physical and mechanical properties of cure thermosets. In the current study, crosslink density is determined from swelling measurements. Table 3 shows the crosslink density of composites produced by mini-extruder and solution mixing for different filler loadings. The crosslink density of PDMS filled with 1 wt% MWCNT-p is the highest. Increasing the nanotube content to 4 wt% reduces the crosslink density of the composite. However, the crosslink density for PDMS/4 wt% MWCNT-p is still higher than that of neat PDMS. Comparing the composites produced by mini-extruder and solution mixing, the crosslink density of M-PDMS/MWCNT-p is higher than that of S-PDMS/MWCNT-p at the same filler content, indicating a poor filler-matrix interface.

It was reported that crosslink density can affect the mechanical properties of composites (18, 19). The effect of crosslink density on the mechanical properties of PDMS/MWCNT-p composites will be discussed in Section 3.3.4.

Table 3: Crosslink density of composites produced by mini-extruder and solution mixing.

Composite	Crosslink Density (mol/cm^3)
PDMS	1.06×10^{-2}
M-PDMS/1 wt% MWCNT-p	3.08×10^{-2}
M-PDMS/4 wt% MWCNT-p	1.78×10^{-2}
S-PDMS/1 wt% MWCNT-p	2.50×10^{-2}
S-PDMS/4 wt% MWCNT-p	1.61×10^{-2}

3.3.3 Thermal Conductivity

The thermal conductivity of PDMS/MWCNT-p composites produced by mini-extruder and solution mixing method as a function of nanotubes content are shown in Figure 3 whereas Table 4 shows the thermal conductivity values for the PDMS composites produced by mini-extruder and solution mixing method as well as the % improvement in comparison to neat PDMS. The thermal conductivity for neat PDMS produced by mini-extruder and solution mixing method are slightly similar, with a value of 0.167 W/m.K and 0.165 W/m.K, respectively. In general, the thermal conductivity for both composites is found to increase almost linearly with nanotubes content. For composites produced by mini-extruder, adding 1 wt%, 2 wt%, 3 wt%, and 4 wt% MWCNT-p into PDMS increases the thermal conductivity by 17%, 25%, 29%, and 38%, respectively. For composites produced by solution mixing, adding 1 wt%, 2 wt%, 3 wt%, and 4 wt% MWCNT-p into PDMS increases the thermal conductivity (in comparison to neat PDMS) by 15%, 21%, 25%, and 36%, respectively. The thermal conductivity increment with filler loading is rather expected due to the fact that the thermal conductivity of MWCNTs is much higher than PDMS. The addition of nanotubes into PDMS, especially at high filler loading increases the overall thermal conductivity of composites because conductive pathways are formed and phonons can be transferred. Phonons, quantized mode of vibration occurring in a

rigid crystal lattice, are the primary mechanism of heat conduction in polymers since free movement of electrons is not possible (20).

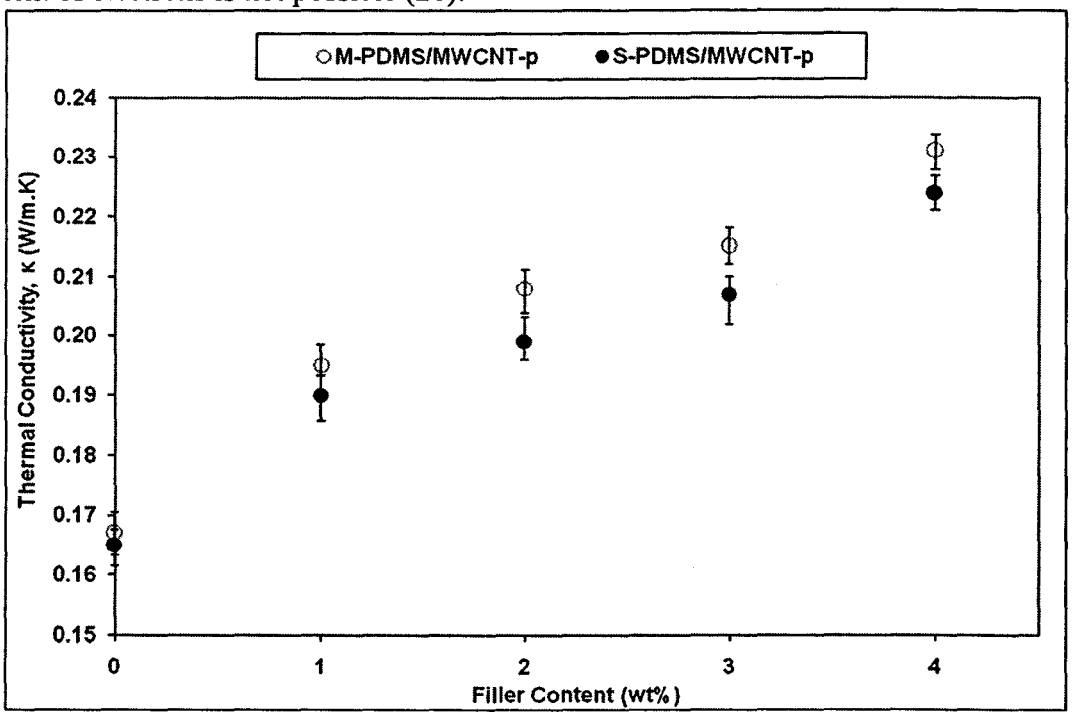

Figure 8: Thermal conductivity of M-PDMS/MWCNT-p and S-PDMS/MWCNT-p as a function of filler loading.

Table 4: Thermal conductivity values of PDMS/MWCNT composites produced by mini-extruder and solution mixing method and the percentage of thermal conductivity improvement.

MWCNT-p	Thermal Conductivity (W/m.K)		Improvement (%)	
(wt%)	Mini-extruder	Solution Mixing	Mini Extruder	Solution Mixing
0	0.167 ± 0.004	0.165 ± 0.003	-	-
1	0.195 ± 0.004	0.190 ± 0.004	17	15
2	0.208 ± 0.004	0.199 ± 0.004	25	21
3	0.215 ± 0.003	0.207 ± 0.004	29	25
4	0.231 ± 0.003	0.224 ± 0.002	38	36

* *The % improvement was compared to the neat PDMS*

For all filler loadings, the thermal conductivity of composites produced by mini-extruder is consistently slightly higher than the ones produced by solution mixing. For composites produced by mini-extruder, adding 4 wt% MWCNT-p into PDMS yields a thermal conductivity of 0.231 W/m.K, whereby an increase of 38% (in comparison to neat PDMS) is observed. On the

other hand, the composites prepared by solution mixing recorded 0.224 W/m.K, with an increase of 36%. The slightly higher thermal conductivity for mini-extruder composites is due to the shorter nanotubes and better nanotubes dispersion in PDMS, as seen in SEM micrographs in Figures 6 and 7. A similar result is obtained by Wang et al. (17) whereby the thermal conductivity of chopped and shortened SWCNT increased the thermal conductivity of epoxy by ~40 % and this is attributed to the improved percolation and interfacial heat transport as a result of better nanotubes dispersion.

3.3.4 Tensile Properties

The tensile test was carried out to study the effect of filler loading and processing methods on the tensile strength, modulus at 50% elongation (M50), and elongation at break of the composites. Table 5 shows the values of tensile strength, M50, and elongation at break of composites produced by mini-extruder (M-PDMS/MWCNT-p) and solution mixing (S-PDMS/MWCNT-p) while Figures 9, 10, and 11 illustrates the tensile strength, M50, and elongation at break, respectively, as a function of filler loading.

From Figures 9 and 10, it can be observed that regardless of the processing method, the tensile strength and M50 of PDMS/MWCNT-p composites are the highest at 1 wt% nanotubes loading. This indicates that 1 wt% is the optimum nanotubes loading within the range of compositions examined here. Further addition of MWCNT-p from 2–4 wt% resulted in a gradual decrease of tensile strength and M50.

Table 5: Values of tensile strength, M50, and elongation at break of PDMS composites.

MWCNT	Tensile Strength (MPa)		M50 (MPa)		Elongation at Break (%)	
(wt%)	Mini-extruder	Solution Mixing	Mini-extruder	Solution Mixing	Mini Extruder	Solution Mixing
0	2.29 ± 0.06	2.17 ± 0.07	0.51 ± 0.06	0.50 ± 0.08	110.50 ± 6.43	113.03 ± 10.02
1	2.62 ± 0.16	2.37 ± 0.26	1.91 ± 0.30	0.97 ± 0.06	55.87 ± 5.08	82.67 ± 6.33
2	2.24 ± 0.16	1.71 ± 0.21	1.65 ± 0.14	0.82 ± 0.03	70.67 ± 5.42	92.67 ± 4.79
3	2.04 ± 0.09	1.62 ± 0.06	1.57 ± 0.11	0.76 ± 0.03	89.46 ± 9.3	99.55 ± 2.31
4	1.99 ± 0.13	1.47 ± 0.15	1.45 ± 0.14	0.64 ± 0.03	104.7 ± 4.65	107.33 ± 5.26

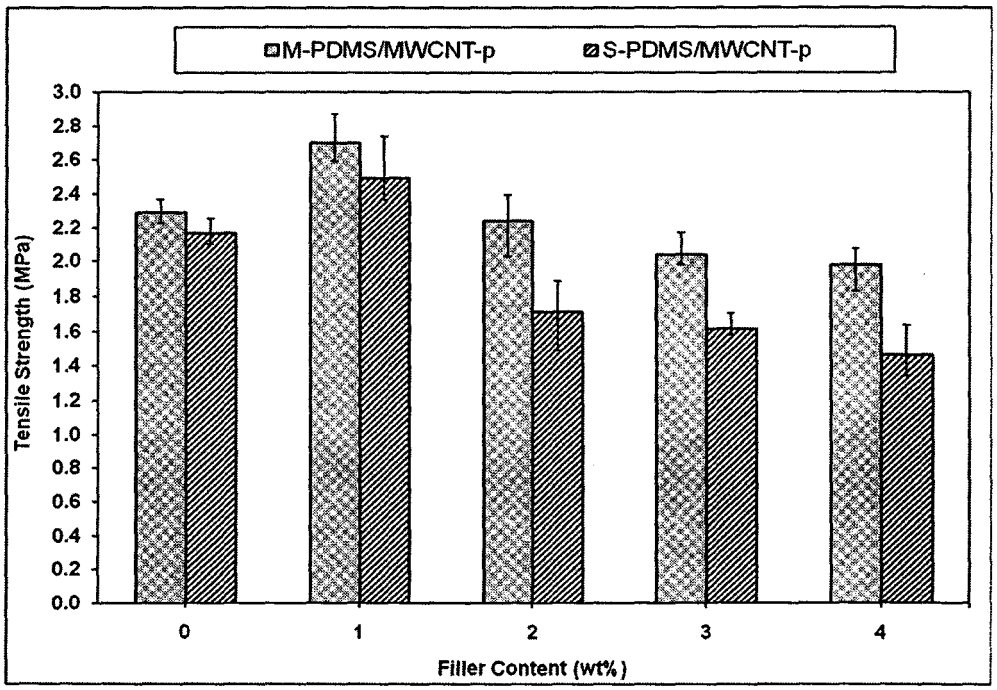

Figure 9: Tensile strength of composite produced by different processing methods as a function of MWCNT loading.

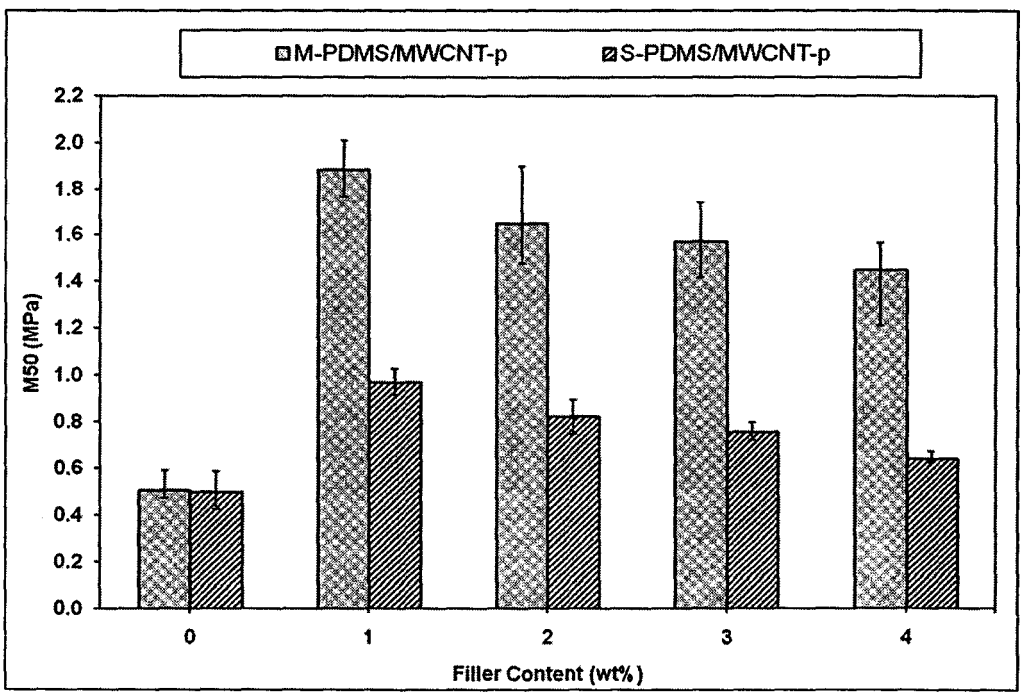

Figure 4.10: Modulus at 50% elongation (M50) of composite produced by different processing methods as a function of MWCNT loading.

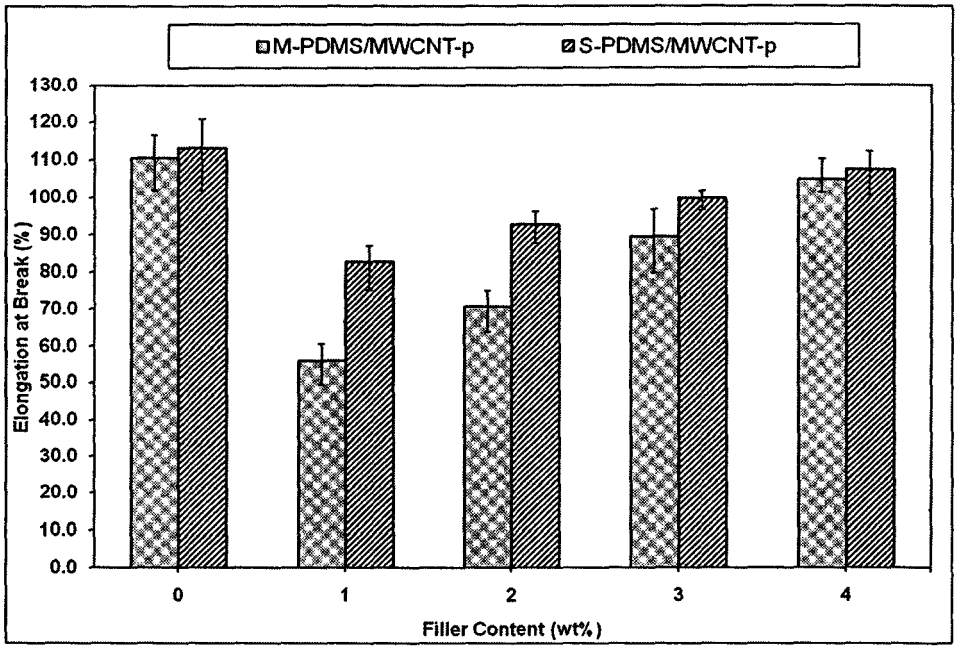

Figure 11: Elongation at break of composite produced by different processing methods as a function of MWCNT loading.

The increase in tensile strength and M50 upon the addition of 1 wt% MWCNT is due to the transfer of stress from PDMS matrix to MWCNTs and the reinforcing effect of MWCNTs, which leads to the increase of tensile strength. The decline in tensile strength and M50 at high filler loading is not unusual as this trend has been reported elsewhere (10, 21). Results by Chua et al. (10) revealed that the tensile strength of PDMS composite decreased about 83% as compared to neat PDMS when 2 vol% of pristine MWCNTs were added into the PDMS. The high surface area of nanotubes increased the viscosity of silicone rubber solution during mixing process and caused the mixing process to become less effective. Table 6 shows the addition of 4 wt% MWCNT-p into PDMS resulted in a high resin viscosity.

Table 6: Viscosity of PDMS/MWCNTs composite mixture during mixing process.

MWCNTs content (wt %)	Viscosity (cP)	
	Mini-extruder	Solution Mixing
0	4320	4570
1	5050	5520
2	6870	7320
3	8990	9960
4	12440	15460

** The viscosity value was measured during composite preparation. For mini-extruder, the viscosity value was obtained directly from the equipped software while for solution mixing, the viscosity was measured using Brookfields Viscometer*

As the filler loading is increased, a level is reached whereby the nanotubes or aggregates are no longer adequately separated or wetted by the rubber phase. This led to the formation of voids and large agglomerates, which prevents efficient load transfer from PDMS matrix to the nanotubes. This subsequently reduces the tensile strength and M50. SEM micrographs in Figures 6(b) and 6(d) reveal the presence of large agglomerates in PDMS/4 wt% MWCNT-p composites. As comparison, only a small fraction of agglomerates can be seen in PDMS/1 wt% MWCNT-p composites, as shown in Figures 6(a) and 6(c). In addition, it was reported that the tensile strength and modulus of rubber vulcanizate is a proportional to the degree of crosslink density. This result can also be related to the findings in Table 3 where the crosslink density of composites with high nanotubes loading is lower than the composites with low filler loading, hence the decreased in tensile strength and M50 (18, 19).

Figure 11 shows the elongation at break plotted as a function of filler loading. The elongation at break decreases when 1 wt% MWCNT-p is added into PDMS. As the MWCNT-p content is increased from 2 – 4 wt%, the elongation at break increases. This trend is consistent with the results of crosslink density obtained in Table 3. Choi et al. (18) reported that the elongation at break of an elastomer with higher crosslink density is lower than that of an elastomer with lower crosslink density since the elongation at break is inversely proportional to the degree of crosslink density. Although the elongation at break increases with MWCNT-p content, it is noted that in general, the elongation at break of filled PDMS is lower than the neat PDMS.

Unfilled PDMS is used as a control in this research. From Table 5, the tensile strength and M50 of unfilled PDMS mixed by mini-extruder is 2.29 MPa and 0.51 MPa, slightly higher than the unfilled PDMS mixed via solution mixing (2.17 MPa and 0.50 MPa). This could be reasoned by the mixing efficiency of mini-extruder where the base resin and curing agent are well-mixed. Comparing the composites prepared by the two different processing methods, the tensile strength and M50 of composites produced by mini-extruder is much higher than the ones prepared via solution mixing method. This result is due to the high shear mixing mechanism of the mini-extruder. The high shear mixing produced sufficient energy to separate and break down the bundles of MWCNTs into smaller aggregates and individual nanotubes. This mixing mechanism also cut the nanotubes into shorter lengths (as proven by SEM micrographs shown in Figure 7), which enabled the nanotubes to be dispersed more easily in the matrix. A good and homogenous dispersion of MWCNTs with minimal agglomerates yields higher tensile strength and M50 but lower elongation at break. SEM observations of the composite fracture surface in Figure 6 shows better nanotube dispersion and smaller aggregates in the mini-extruder-produced composites. In contrast, lumps and large agglomerates of nanotubes can be seen in the samples produced via solution mixing method. As for the elongation at break, composites produced by solution mixing elongates longer than the composites produced by mini-extruder. Again, this is attributed to the lower crosslink density of composites produced by solution mixing. Composites with lower crosslink density will elongate longer than composites with higher crosslink density (18).

3.3.5 Electrical Conductivity

Figure 12 shows the changes in electrical conductivity of the composite samples as a function of nanotube content. The conductivity of the solution mixed composite (S-PDMS/MWCNT-p) increases from 1.25 x 10^{-10} S/m to 9.81 x 10^{-6} S/m when 1 wt% MWCNT-p is added into PDMS, indicating a formation of percolating network. The electrical conductivity continues to increase to 1.83 x 10^{-3} S/m when 4 wt% MWCNT-p is added. As for the composites produced by mini-extruder (M-PDMS/MWCNT-p), the electrical conductivity increases from 1.25 x 10^{-10} S/m to 1.53 x 10^{-6} S/m with the addition of 4 wt% MWCNT-p. The enhancement in electrical conductivity with the addition of nanotubes is expected because it obeys the percolation theory. As the MWCNT-p content increases, the high aspect ratio of nanotubes forms conductive networks. These conductive networks act as pathways for the electrons to move, thus giving rise to the composites electrical conductivity.

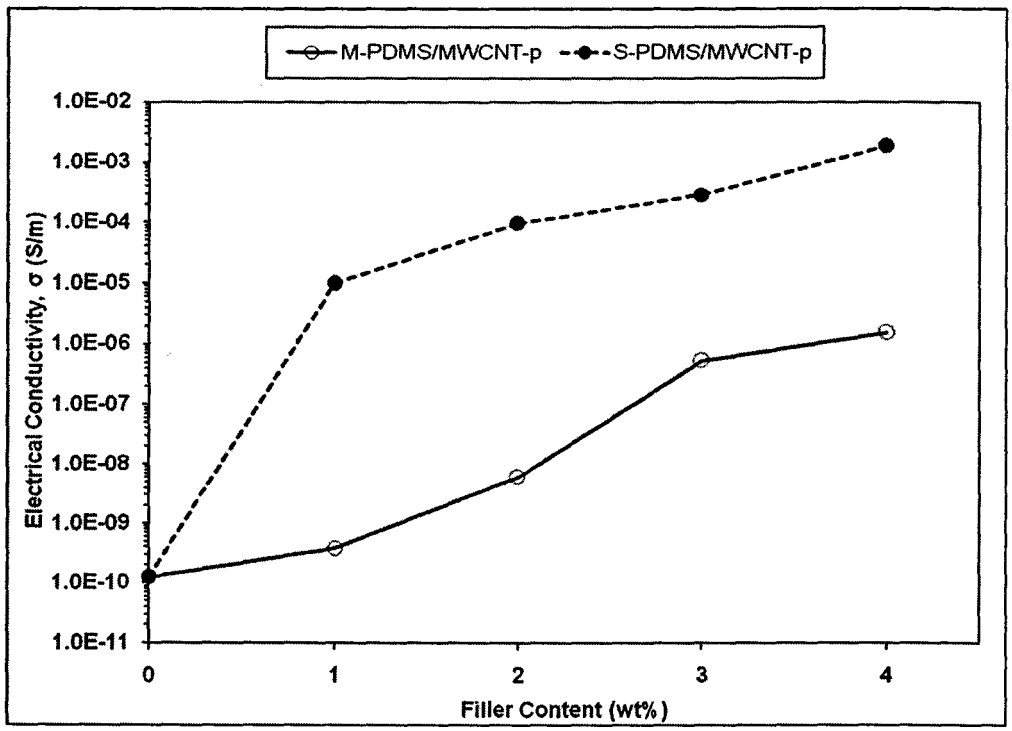

Figure 12: Electrical conductivity as a function of filler loading for composites produced by mini-extruder and solution mixing method.

In general, the composites produced by solution mixing method are electrically more conductive than the composites produced by mini-extruder. The electrical conductivity of the solution mixed composite (S-PDMS/CNT) increases sharply by four orders of magnitude when only 1 wt% nanotubes is added into PDMS. In contrast, the conductivity of the mini-extruder-produced composite (M-PDMS/CNT) increased less sharply by three orders of magnitude with the addition of 1–3 wt% nanotubes. Bai and Allaoui (22) pointed out that electrical conductivity of filled composite sharply increases when a conductive path of interconnected nanotubes is formed through the volume of the sample. They compared the effect different MWCNTs length on the electrical conductivity of epoxy composites. Nanotubes with longer lengths possess higher

probability to form aggregate and conductive networks and subsequently increase the electrical conductivity of the composites. In this study, the high shear mixing mechanism of the mini-extruder cut the nanotubes into shorter ones, thus, greatly reducing the ability to form a conductive path and network despite good dispersion. Although there is no specific data to support the existence of nanotubes length and aspect ratio reduction for the mini-extruder-produced samples, SEM micrographs in Figure 4.8 clearly shows a significant difference in nanotubes length between the composites produced by two different methods. It was said that measuring the length of CNT within the polymer matrix is neither a common nor easy task.

3.3.6 Thermal Stability

The thermal stability of composites was analyzed using thermogravimetry analysis (TGA) and the curves obtained are shown in Figure 13. Table 7 presents the decomposition temperature at 5% (T_5) and 10% (T_{10}) weight loss as well as weight remaining at 800 °C for PDMS/MWCNT composites.

The T_5 of unfilled PDMS produced by mini-extruder and solution mixing are 350 °C and 354 °C, respectively. Adding 1 wt% of MWCNT-p shifts the T_5 of the composites higher by 23 °C for the mini-extruder sample and 27 °C for the solution mixed sample while adding 4 wt% of MWCNT-p increases the T_5 of the composites higher by 40 °C for the mini-extruder sample and 51 °C for the solution mixed sample. This indicates that the presence of CNT enhances the thermal stability of PDMS composites. With increasing nanotubes contents, the enhancement of thermal stability is even greater. Such behavior has also been reported elsewhere (10, 21) reported thermal stability enhancement in poly(ethylene 2,6-naphthalte) (PEN) with the addition of 0.5 wt% MWCNT, indicating the presence of nanotubes could lead to stabilization of PEN matrix and enhancement of thermal stability of PEN composites. The nanotubes can effectively act as physical barriers to prevent the transport of volatile decomposed products out of the PEN composites during thermal decomposition.

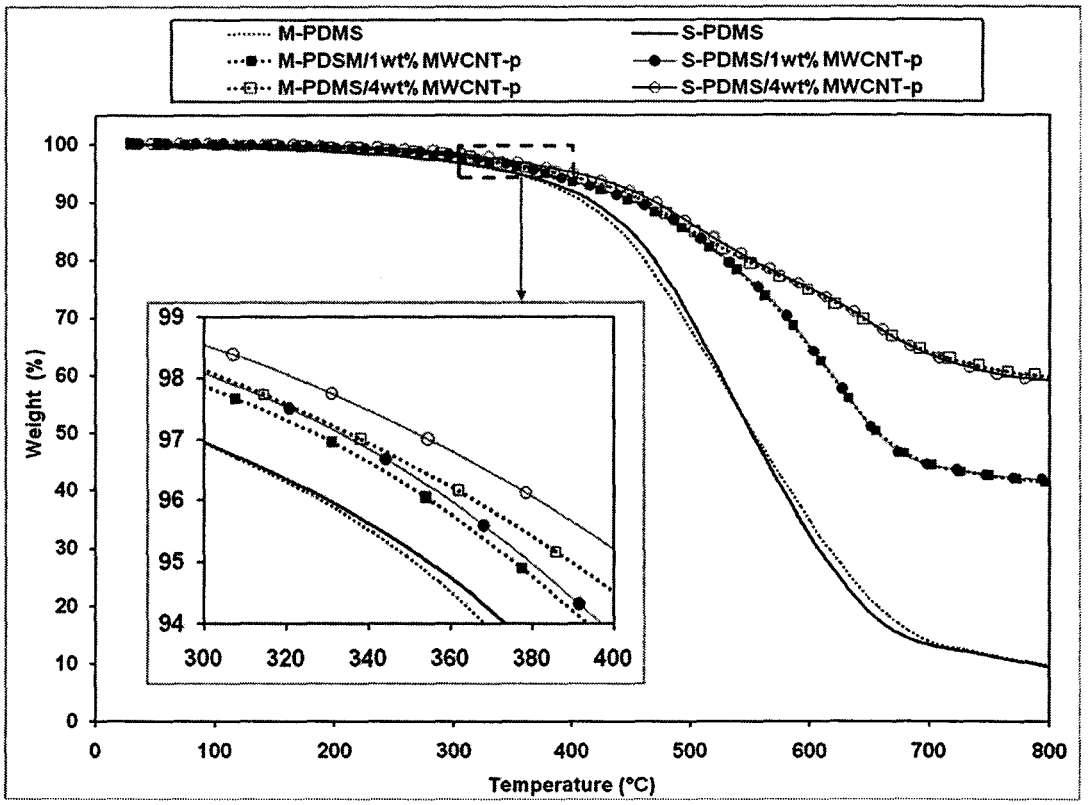

Figure 13: Thermogravimetric curves for composites produced by mini-extruder and solution mixing, obtained in nitrogen atmosphere. *Inset:* Enlarged curves from the range of 300 °C – 400 °C.

Table 7: Thermal stability data for PDMS/MWCNT-p composites extracted from TGA curves.

Sample	T_5 (°C)		T_{10} (°C)		Residue at 800 °C (%)	
	Mini-extruder	Solution Mixing	Mini extruder	Solution Mixing	Mini-extruder	Solution Mixing
PDMS	350	353	410	418	9.8	9.6
PDMS/1 wt% MWCNT-p	373	380	452	457	41.3	41.7
PDMS/4 wt% MWCNT-p	390	404	465	481	59.8	59.2

**T_5 and T_{10} represents decomposition temperature at 5% and 10% weight loss, respectively*

The solution mixed composites have higher T_5 and T_{10} compared to the ones produced by mini-extruder at the same filler content, hinting that these samples are more thermally stable. The

T_5 of solution mixed composites with 4 wt% MWCNT-p are about 14 °C higher than the mini-extruder composites. This is because the nanotubes in solution-mixed samples were able to maintain its high aspect ratio whereas the nanotubes in mini-extruder samples have reduced aspect ratio, as discussed previously in Section 3.3.1. The relatively higher aspect ratio of the nanotubes in solution mixing method could have retarded the diffusion and extravasations of small molecules from matrix under high temperature, leading to a increased decomposition temperature.

Table 7 shows that the amount of residues at 800 °C for neat PDMS mixed with mini-extruder and solution mixing are 9.8% and 9.6%, respectively. Adding 1 wt% of MWCNT-p increases the residues of composites to 41.3% and 41.7%, respectively while adding 4 wt% of MWCNT-p increases the residues of composites to 59.8% and 59.2%, respectively. This shows that higher content of nanotubes in composites will produce higher amount of residues. The obtained residues are believed to be nanotubes. Pristine carbon nanotubes are thermally stable in nitrogen environment even at elevated temperature of 800 °C. TGA analysis in Table 2 has proven that MWCNT-p are thermally stable at 800 °C. For neat PDMS, the residue amount is around 10%. Since the TGA is done in inert atmosphere, the obtained residue could most probably be due to the formation of ceramic type of structure.

3.3.7 Coefficient of Thermal Expansion

The coefficient of thermal expansion (CTE) is used to quantify the thermal expansion of a solid. The coefficient can be volumetric or linear depending on whether the measurement is determined by the change of volume or length of the sample (Wang et al., 2007a). In the current research, CTE is tested through TMA and measured according to the change of length, hence giving a linear CTE. From the expansion-temperature curve obtained from TMA, the glass transition temperature (T_g) can be calculated as well. It is determined by the dramatic turning point on the expansion-temperature curve. CTE can be divided into two parts: CTE below T_g and CTE above T_g. Table 8 lists the results of T_g, CTE below T_g and CTE below T_g measurements for M-PDMS/MWCNT-p and S-PDMS/MWCNTs.

The T_g of PDMS composites shows a very clear trend, that is increasing with the addition of MWCNT-p. For composites produced by mini-extruder, the T_g increases from -88.5 °C in neat PDMS to -78.8 °C in PDMS/1 wt% MWCNT-p, an increase of 9.7 °C. Similarly for composites produced via solution mixing, the T_g increases from -89.1 °C in neat PDMS to -81.2 °C in PDMS/1 wt% MWCNT-p, an increase of 7.9°. The increasing trend of T_g is similar to the result obtained by Chua (10). On a different matrix system, the T_g of epoxy is also found to increase upon the addition of nanotubes. Wei et al. (23) reasoned that the nanotubes in the matrix tend to slow the motions of the surrounding molecules below T_g and it is possible that the cross-linking of polymer matrix with embedded CNTs may further reduce the motions of polymer molecules which subsequently increase the T_g.

In general, the T_g obtained for composites produced by mini-extruder are higher than the T_g for obtained for composites produced by solution mixing. The T_g for M-PDMS/1 wt% MWCNT-p is -78.8 °C, which is 2.4 °C higher than S-PDMS/1 wt% MWCNT-p's -81.2 °C. The

T_g for M-PDMS/4 wt% MWCNT-p is -82.2 °C, which is 3.2 °C higher than S-PDMS/4 wt% MWCNT-p's -85.4 °C. The higher T_g for M-PDMS/MWCNT-p composites is mainly due to the relatively better dispersion of nanotubes and lesser nanotubes agglomerations in M-PDMS/MWCNT-p composites. When the nanotubes are well dispersed in PDMS matrix, the mobility restriction of PDMS macromolecules is higher and hence, results in higher T_g.

Table 8: Values of T_g and CTE for composites produced by mini-extruder and solution mixing.

Sample	T_g (°C)		CTE below T_g (x 10^{-6}/°C)		CTE abovc T_g (x 10^{-6}/°C)	
	Mini-extruder	Solution Mixing	Mini extruder	Solution Mixing	Mini-extruder	Solution Mixing
PDMS	-88.5	-89.1	79.0	79.9	330.2	335.7
PDMS/1 wt% MWCNT-p	-78.8	-81.2	31.8	52.2	340.4	354.3
PDMS/4 wt% MWCNT-p	-82.2	-85.4	54.5	72.7	360.5	435.0

Figures 14 and 15 shows the CTE values below and above T_g as a function of filler loading, respectively for M-PDMS/MWCNT-p and S-PDMS/MWCNTs. The CTE trend as a function of filler loading for composite below T_g is completely the opposite of the composite above T_g. Interestingly, the CTE values of composites produced by mini-extruder is consistently lower than the ones produced via solution mixing.

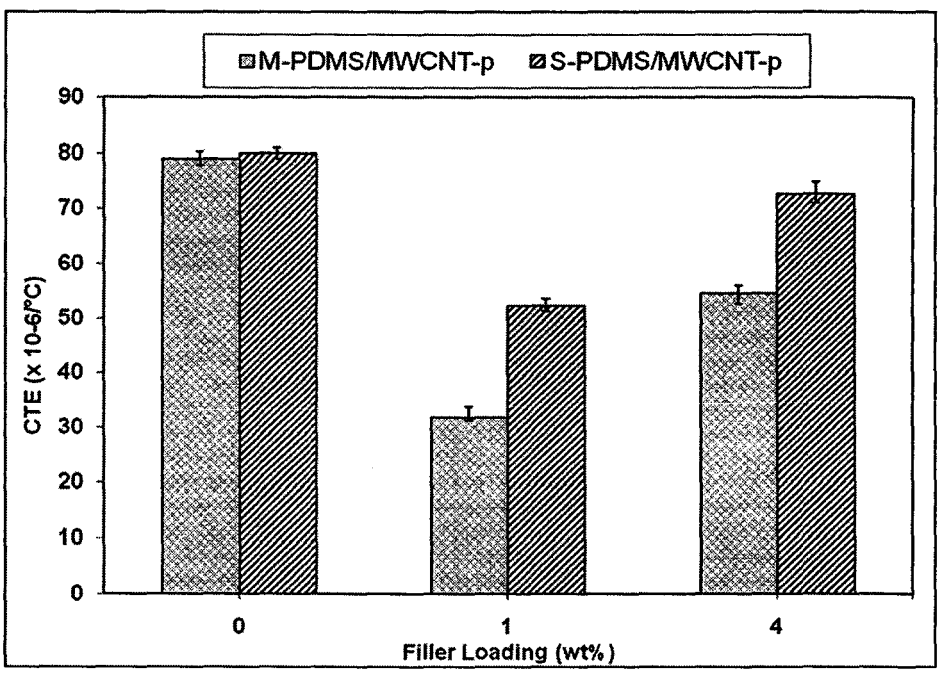

Figure 14: CTE values of M-PDMS/MWCNT-p and S-PDMS/MWCNT-p below the T_g range.

From Figure 15, it is observed that the CTE below T_g of composites decreases when MWCNT-p are added to PDMS. For composites produced by mini-extruder, the CTE below T_g reduces 59.8% and 31.0% when 1 wt% and 4 wt% MWCNT-p are added into PDMS, respectively. For composites produced via solution mixing method, the CTE below T_g reduces 34.7% and 9.0% when 1 wt% and 4 wt% MWCNT-p are added into PDMS. The reduction of CTE below T_g is in agreement with previous reported works (17, 24). Wang et al. (17) reported a reduction of about 27% in CTE below T_g when 1 wt% of SWCNT was added into epoxy. Molecular dynamics (MD) simulations by Wei (23) suggest that CTE of MWCNTs is negative because of thermal contraction. Thus, the addition of MWCNT into PDMS will result in a decrease of CTE value. Comparing the composites produced by two different processing methods, the CTE reduction for M-PDMS/1 wt% MWCNT-p is significantly higher than S-PDMS/1 wt% MWCNT-p. This could be due to the better dispersion of M-PDMS/1 wt% MWCNT-p as observed in Figure 15. Wang et al. (17) suggested that CTE is also dependent on nanotube dispersion where a better dispersion will reduce the CTE significantly.

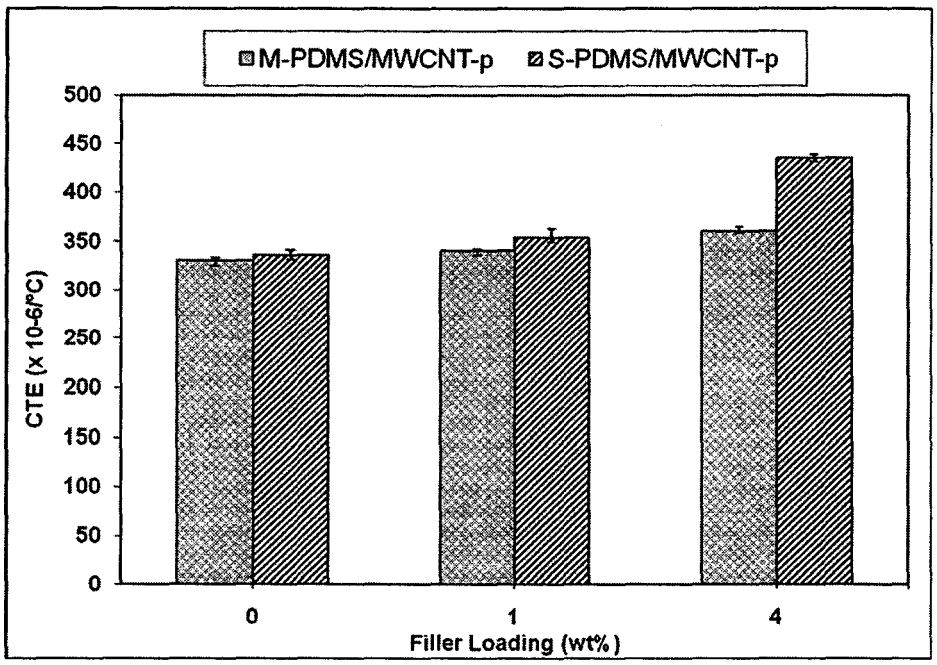

Figure 15: CTE values of M-PDMS/MWCNT-p and S-PDMS/MWCNT-p above the T_g range.

As for composites above T_g, the CTE increases upon addition of MWCNT-p. Figure 4.16 shows that the CTE values for all composites are higher than that of neat PDMS even though MWCNTs have negative CTE values. These results are consistent with the results of Chua (10). Wei et al. (23) attributed these CTE increments above T_g range to the phonon modes vibration and Brownian motion of the nanotubes. The MWCNTs embedded within a polymer matrix have a fixed volume and exclude the occupancy of the polymer chains. The excluded volume of the embedded nanotubes will increase with increasing temperature. This increase of excluded

volume will subsequently increase the CTE at temperature above T_g. However, the magnitude of CTE increment differs according to the processing methods used to produce composites. Adding 4 wt% MWCNT-p into PDMS increases the CTE of M-PDMS/MWCNT-p and S-PDMS/MWCNT-p by 9.2% and 29.6%, respectively. As reported earlier, the high shearing mixing mechanism of mini-extruder had chopped the nanotubes into shorter lengths. The chopped nanotubes could have both ends opened. The PDMS and curing agent had the chance to enter the tubes, resulting in a mechanical locking nanostructure, which confined the thermal vibration and Brownian motion of the nanotubes by a dense crosslinked network. As a result, the magnitude of increase excluded volume of MWCNT with increasing temperature is minimum and the CTE enhancement is also low (17).

3.3.8 Dynamic Mechanical Properties

The effect of MWCNT-p on the dynamic mechanical properties of PDMS composites was analyzed by DMA. Two important characteristics that can be obtained from DMA are stiffness, which is reported as storage modulus (E') and damping, which is reported as loss factor (tan δ). The storage modulus measures the sample's elastic material while the loss factor measures the energy dissipation of a material. Another characteristic that can be obtained from DMA is the glass transition temperature (T_g). Table 8 compares the values of storage modulus at 130 C°, peak height of tan δ, and the corresponding T_g for M-PDMS/MWCNT-p and S-PDMS/MWCNT-p composites.

Table 8: Values of storage modulus at -130 °C, peak height of tan δ, and the corresponding T_g for composites produced by mini-extruder and solution mixing.

Sample	Storage modulus at -130 °C, E' (MPa)		Peak Height of Tan δ		T_g (°C)	
	Mini-extruder	Solution Mixing	Mini extruder	Solution Mixing	Mini-extruder	Solution Mixing
PDMS	361	341	0.2958	0.3025	-55.9	-55.9
PDMS/1 wt% MWCNT-p	542	481	0.2408	0.2405	-40.8	-48.8
PDMS/4 wt% MWCNT-p	752	645	0.2306	0.2349	-42.6	-49.9

* *The storage modulus value is taken at -130 °C because this is the lowest temperature that can be achieved in this experiment.*

The T_g obtained from the tan δ peak position for M-PDMS/MWCNT-p composites is consistently higher than that of S-PDMS/MWCNT-p. As been discussed in TMA analysis (Section 3.3.7), this is mainly due to the better dispersion of nanotubes and lesser nanotubes agglomerations in M-PDMS/MWCNT-p composites. When the nanotubes are well dispersed in

PDMS matrix, the mobility restriction of PDMS macromolecules is higher and hence, results in higher T_g. In addition, for composites produced by both methods, the T_g increases with increasing nanotubes content. This is in accordance to the results obtained from TMA, as discussed in Section 3.3.7.

Figure 16 shows the storage modulus of neat PDMS and PDMS composites, characterized as a function of temperature. It is found that the storage modulus of the PDMS/MWCNT-p composites is higher than that of the neat PDMS. The addition of 1 wt% MWCNT-p and 4 wt% MWCNT-p increases the storage modulus at temperature below T_g. Interestingly, there is little effect on the storage modulus of PDMS at temperature above T_g. when MWCNT-p is added. The increment in storage modulus upon addition of nanotubes has been reported by Chua et al. (10). The increment in storage modulus is attributed to the high modulus and specific surface areas of MWCNT-s, which enhance the stiffness of PDMS and subsequently increase the storage modulus of composites (25). In comparison, the composites produced by mini-extruder have higher storage modulus than the composites produced by solution mixing, especially at temperature below T_g. The much better dispersion of nanotubes in composites produced by mini-extruder could have contributed to the high values of storage modulus.

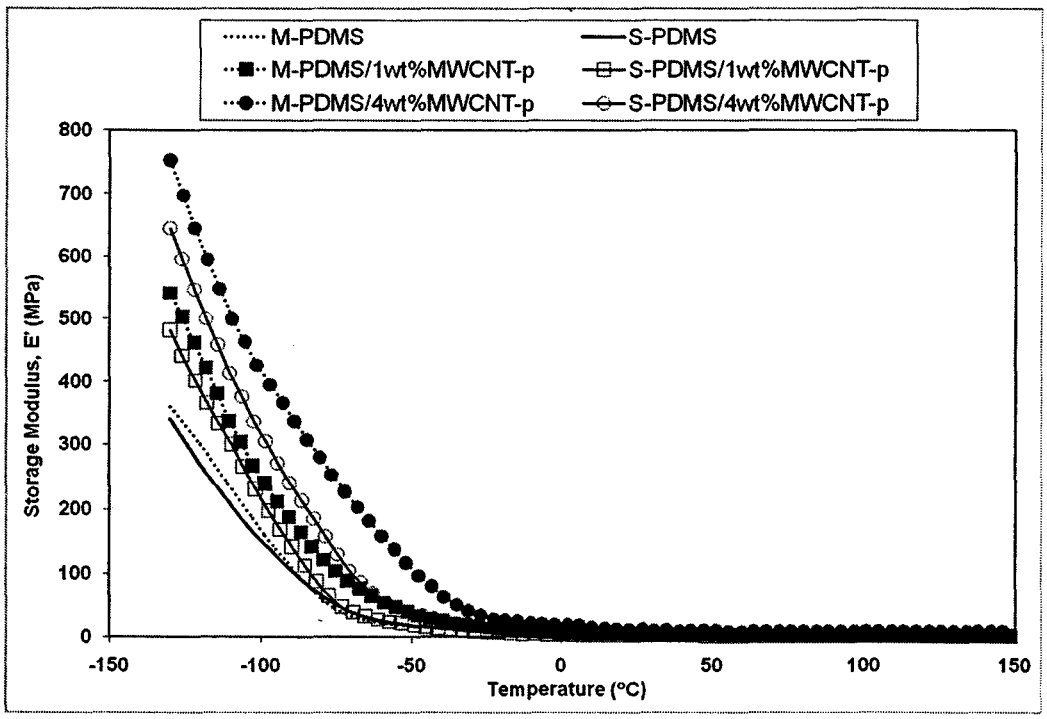

Figure 16: Storage modulus as a function of temperature for composites produced by mini-extruder and solution mixing at various MWCNT-p loadings.

The tan δ as a function of temperature for composites produced by mini-extruder and solution mixing at various MWCNT-p loadings is shown in Figure 17. From the figure, it can be observed that the peak height of tan δ curve decreases with higher MWCNT-p content. The tan δ value of composites depends on the characteristics of both PDMS and MWCNT-p. The addition of nanotubes reduces the percentage of the PDMS in composites, which lowers hysteresis loss of

the elastomer under oscillating force. Hence, the peak height of tan δ decreases after adding the MWCNT-p (25). The peak height of tan δ is almost similar for both processing methods.

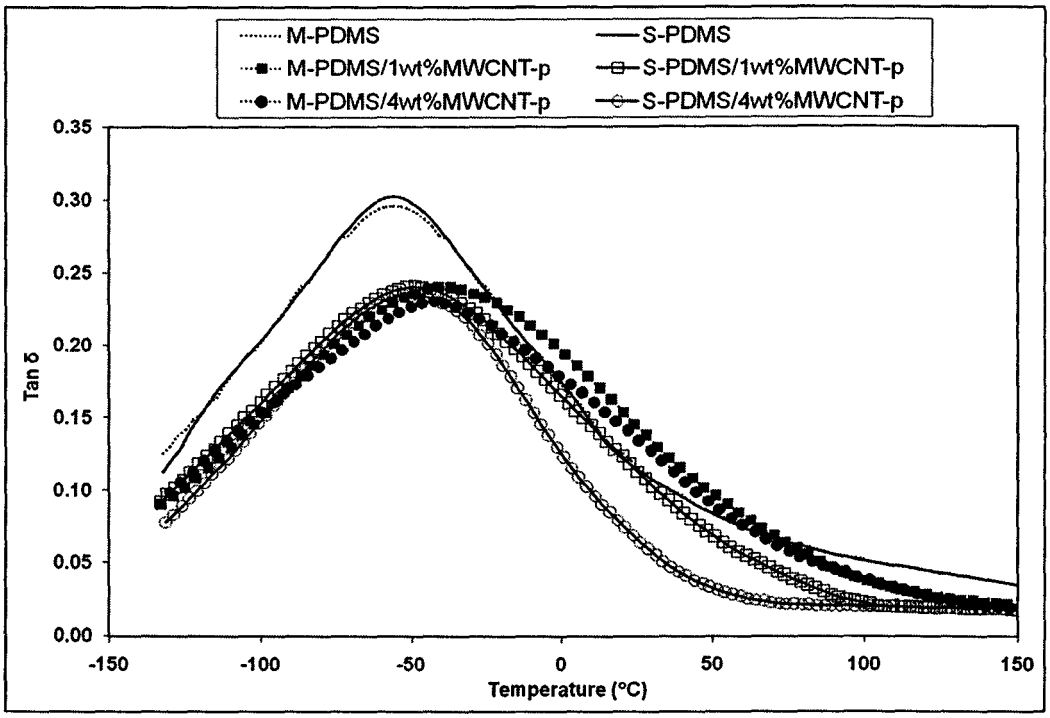

Figure 17: Tan δ as a function of temperature for composites produced by mini-extruder and solution mixing at various MWCNT-p loadings.

The position of tan δ peak in the curve can be used to identify the T_g of the composite materials. Adding 1 wt% and 4 wt% of MWCNT-p into PDMS slightly shifts the position of the tan δ peak to a higher temperature compared to that of the neat PDMS. This indicates that the T_g of composites increases with filler loading and this corresponds with the results from TMA as well. The increment shows that the mobilization of the PDMS macromolecules is restricted due to the presence of nanotubes (25).

4. Conclusions

Major findings from the results of this study are highlighted below:

1) SEM micrographs of fracture surface reveal that composites produced by mini-extruder have very good and homogenous dispersion as compared to the ones produced by solution mixing; however, this advantage comes at a cost: reduction of nanotubes length and aspect ratio. Thus, this processing method only benefits certain properties, such as thermal conductivity, tensile strength and storage modulus. For example, the thermal conductivity of M-PDMS/4 wt% MWCNT-p increases 38% as compared to 36% for S-PDMS/4 wt% MWCNT-p whereas the tensile strength of M-PDMS/1 wt% MWCNT-p increases 14% as compared to 9% for S-PDMS/1 wt% MWCNT-p. On the other hand,

the solution mixing method does not heavily damage or reduce the nanotubes length, thereby preserving the high aspect ratio of nanotubes. This method does not promote nanotubes dispersion as good as that of the former; however, the high aspect ratio of nanotubes compensates the drawback by enhancing the composite electrical conductivity and thermal stability. The electrical conductivity of S-PDMS/4 wt% MWCNT-p increases 7 orders of magnitude while the electrical conductivity of M-PDMS/4 wt% MWCNT increases only 4 orders of magnitude.

2) Functionalization of MWCNTs with either –OH or –COOH group helps improve interfacial adhesion between MWCNTs and PDMS matrix via hydrogen bond, which subsequently improves the thermal conductivity, tensile strength, storage modulus, CTE, glass transition temperature, and thermal stability of the composites. However, functionalization of MWCNTs has very little or no effect on the electrical conductivity. The thermal conductivity of S-PDMS/4 wt% MWCNT-OH increases about 46% as as compared to 36% for S-PDMS/4 wt% MWCNT-p. The tensile strength of S-PDMS/MWCNT-OH increases 51% as compared to 9% for S-PDMS/4 MWCNT-OH. Adding 4 wt% MWCNT-OH increases the electrical conductivity of PDMS composite by 5 orders of magnitude while adding 4 wt% MWCNT-COOH has no effect on the electrical conductivity of PDMS composite.

REFERENCES

1. Sim, L. C., Ramanan, S. R., Ismail, H., Seetharamu, K. N. and Goh, T. J. (2005). Thermal characterization of Al2O3 and ZnO reinforced silicone rubber as thermal pads for heat dissipation purposes. *Thermochimica Acta,* 430(1-2), pp. 155-165.

2. Zhao, Y. F., Xiao, M. and Wang, S. J. (2007). Preparation and properties of electrically conductive PPS/expanded graphite nanocomposites. *Composites Science and Technology,* 67(11/12), pp. 2528-2534.

3. Zhou, Z., Wang, S., Lu, L., Zhang, Y. and Zhang, Y. (2008b). Functionalization of multi-wall carbon nanotubes with silane and its reinforcement on polypropylene composites. *Composites Science and Technology,* 68(7-8), pp. 1727-1733.

4. Li, Q., Yan, H., He, M. and Liu, Z. (2004). Thionine-mediated chemistry of carbon nanotubes. *Carbon,* 42(2), pp. 287-291.

5. Yue, D., Liu, Y., Shen, Z. and Zhang, L. (2006). Study on preparation of carbon nanotubes/rubber composites. *Journal of Materials Science,* 41(8), pp. 2541-2544.

6. Bokobza, L. (2008). Mechanical, electrical, spectroscopic investigations of carbon nanotube-reinforced elastomers. *Vibrational Spectroscopy,* 51(1), pp. 52-59.

7. Das, A., Stockelhuber, K., Jurk, R., Saphiannikova, M., Fritzsche, J., Lorenz, H., et al. (2008). Modified and unmodified multiwalled carbon nanotubes in high performance solution-styrene–butadiene and butadiene rubber blends. *Polymer,* 49(24), pp. 5276-5283.

8. Wu, C.-L., Lin, H.-C., Hsu, J.-S., Yip, M.-C. and Fang, W. (2009). Static and dynamic mechanical properties of polydimethylsiloxane/carbon nanotube nanocomposites. *Thin Solid Films,* 517(17), pp. 4895-4901.

9. Hong, J., Lee, J., Hong, C. K. and Shim, S. E. (2010). Effect of dispersion state of carbon nanotube on the thermal conductivity of poly(dimethyl siloxane) composites. *Current Applied Physics,* 10(1), pp. 359-363.

10. Chua, T. P., Mariatti, M., Azizan, A. and Rashid, A. A. (2010). Effects of surface-functionalized multi-walled carbon nanotubes on the properties of poly(dimethyl siloxane) nanocomposites. *Composites Science and Technology,* 70(4), pp. 671-677.

11. Xing, Y., Li, L., Chusuei, C. C. and Hull, R. V. (2005). Sonochemical Oxidation of Multiwalled Carbon Nanotubes. *Langmuir,* 21(9), pp. 4185-4190.

12. Kim, J. Y. (2009). Carbon Nanotube-Reinforced Thermotropic Liquid Crystal Polymer Nanocomposites. *Materials,* 2(4), pp. 1955-1974.

13. Bandarian, M., Shojaei, A. and Rashidi, A. M. (2011). Thermal, mechanical and acoustic damping properties of flexible open-cell polyurethane/multi-walled carbon nanotube foams: effect of surface functionality of nanotubes. *Polymer International,* 60(3), pp. 475-482.

14. Musumeci, A. W., R.Waclawik, E. and Frost, R. L. (2008). A comparative study of single-walled carbon nanotube purification techniques using Raman spectroscopy. *Spectrochimica Acta A,* 71(1), pp. 140-142.

15. Li, X., Zhu, H., Jiang, B., Ding, J., Xu, C. and Wu, D. (2003). High-yield synthesis of multi-walled carbon nanotubes by water-protected arc discharge method. *Carbon,* 41(8), pp. 1664-1666.

16. Amr, I. T., Al-Amer, A., Thomas, S., Al-Harthi, M., Girei, S. A., Sougrat, R., et al. (2011). Effect of acid treated carbon nanotubes on mechanical, rheological and thermal properties of polystyrene nanocomposites. *Composites Part B: Engineering,* 42(6), pp. 1554-1561.

17. Wang, S., Liang, R., Wang, B. and Zhang, C. (2009a). Dispersion and thermal conductivity of carbon nanotube composites. *Carbon,* 47(1), pp. 53-57.

18. Choi, S.-S., Park, B.-H. and Song, H. (2004). Influence of filler type and content on properties of styrene-butadiene rubber (SBR) compound reinforced with carbon black or silica. *Polymers for Advanced Technologies,* 15(3), pp. 122-127.

19. Matthew, G., Singh, R. P., Lakshminarayanan, R. and Thomas, S. (1996). Use of natural rubber prophylactics waste as a potential filler in styrene–butadiene rubber compounds. *Journal of Applied Polymer Science,* 61(11), pp. 2035-2050.

20. Han, Z. and Fina, A. (2011). Thermal conductivity of carbon nanotubes and their polymer nanocomposites: A review. *Progress in Polymer Science,* 36(7), pp. 914-944.

21. Chen, X., Wang, J., Lin, M., Zhong, W., Feng, T., Chen, J., et al. (2008). Mechanical and thermal properties of epoxy nanocomposites reinforced with amino-functionalized multi-walled carbon nanotubes. *Materials Science and Engineering A,* 492(1-2), pp. 236-242.

22. Bai, J. and Allaoui, A. (2003). Effect of the length and the aggregate size of MWNTs on the improvement efficiency of the mechanical and electrical properties of nanocomposites—experimental investigation. *Compos Part A: Appl S,* 34(8), pp. 689-694.

23. Wei, C., Srivastava, D. and Cho, K. (2002). Thermal expansion and diffusion coefficients of carbon nanotube-polymer composites. *Nano Letters,* 2(6), pp. 647-650.

24. Qiu, J., Zhang, C., Wang, B. and Liang, R. (2007). Carbon nanotube integrated multifunctional multiscale composites. *Nanotechnology,* 18(27), pp. 275708.

25. Sui, G., Zhong, W. H., Yang, X. P., Yu, Y. H. and Zhao, S. H. (2008). Preparation and preperties of natural rubber composites reinforced with pretreated carbon nanotubes. *Polymers for Advanced Technologies,* 19(11), pp. 1543-1549.